Tests of Wooden Cleats Oriented Along Fibre

Gustafsson, Per-Johan

2008

Document Version:
Publisher's PDF, also known as Version of record

LUND UNIVERSITY

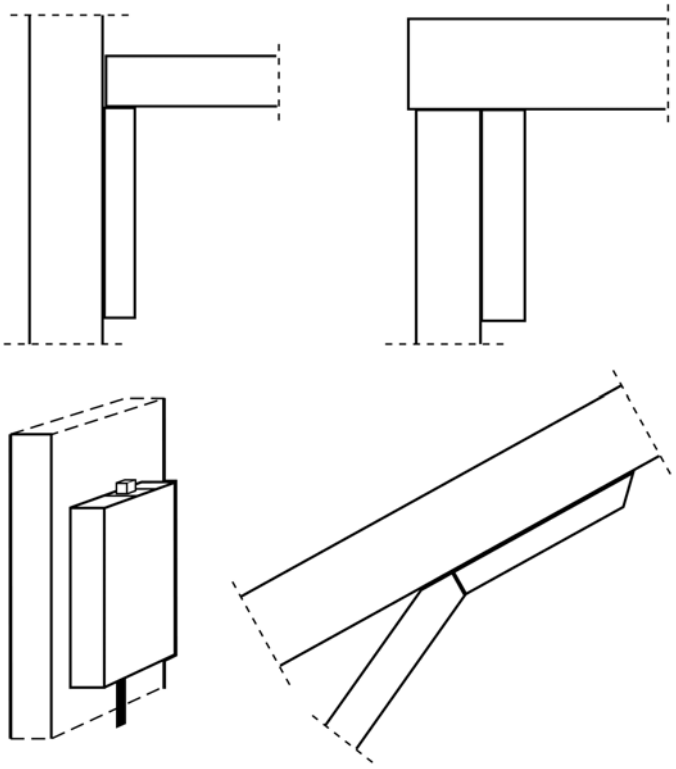

TESTS OF WOODEN CLEATS ORIENTED ALONG FIBRE

PER JOHAN GUSTAFSSON

Structural Mechanics

Department of Construction Sciences
Structural Mechanics

ISRN LUTVDG/TVSM--08/7155--SE (1-67)
ISSN 0281-6679

TESTS OF WOODEN CLEATS ORIENTED ALONG FIBRE

PER JOHAN GUSTAFSSON

Printed by KFS i Lund AB, Lund, Sweden, May 2008.

For information, address:
Division of Structural Mechanics, LTH, Lund University, Box 118, SE-221 00 Lund, Sweden.
Homepage: http://www.byggmek.lth.se

Table of contents

Summary

The strength of wooden cleats glued to glulam columns and oriented along the grain of the glulam was tested. The tests comprised 19 series with 3, 4 or 6 nominally equal tests in each series. The tests series related to various cleat sizes, various cleat lengths to depth ratios, various loading conditions, the effect of screws and the effect of a varying climate condition.

Good load bearing capacity was found for long cleats, about 1000 mm or more in length. The load capacity was for these long cleats not found to be significantly effected by a change of cleat length to depth ratio nor by a change of column size. The mean failure loads were about 250-280 kN for the presently tested 115 mm wide cleats, corresponding to a mean shear stress along the bond line of about 2.0-2.2 MPa. Good load capacity was also found for loading that involved a compressive load component perpendicular to grain.

Poor load capacity was found for cleats with a low length to depth ratio, 3, and for loading that involved a small tensile load component perpendicular to grain.

A wetting-drying moisture cycle including conditioning at 90 % RH for 2 months and then about 30 % RH for 2.5 months gave about 25 % decrease in strength for the tested reference cleats.

Most cleats were both glued and screwed to the column, the purpose of the screws being to give pressure and fixing while the glue hardens. It was found that the screws them self did not contribute to the load capacity, but the cleats that were glued by means of screws had higher strength, at least before the wetting-drying cycle of the specimens.

Fracture developed in almost all specimens tested in the wood along the bond line. For cleats located at the very top of the column it was found that fracture could developed as a perpendicular to grain tensile fracture in the column, not in the vicinity of the bond line.

Placing of the cleat at the long-side of the glulam column cross section did not change the load capacity significantly as compared to placing at the short-side.

Completing tests verified strong sensitivity in load bearing capacity to a load component perpendicular to the cleat. This sensitivity is such that a small resistance to rolling in a not theoretically ideal roller support at the point of load application may affect the load capacity significantly.

Theoretical strength analyses were made by two 1D theories in which only the bond area shear stress, not any perpendicular to grain normal stress, was considered. It was found that such theories are not sufficiently accurate for general application to cleats. A comparison between the test results and a strength design recommendation for glued lap joints showed that the recommendation in general overestimates the strength of cleats, in some cases very much.

Acknowledgements

The tests of cleats presented in this report were financed by The Swedish Glulam Manufacturers Association (Svenskt Limträ AB) and carried out summer and autumn 2007 at Lund University. A few completing tests for verification were made in February 2008 by means of support from an ERDF funding, “Flervåningsbyggander i trä”. The testing work was carried out by Per-Olof Rosenkvist, Konstruktionstekniska laboratoriet.

Special thanks also to Roberto Crocceti, Moelven Töreboda AB, Töreboda, Arne Emilsson, Limträteknik i Falun AB, Falun, Johan Fröbel, Svenskt Limträ AB, Stockholm, and Rune Karlsson, Setra Trävaror AB, Långshyttan, for initiatives and discussions during the planning of the project, organizing administrative matters and organizing manufacture of the test specimens.

March 2008
Per Johan Gustafsson

1. Introduction

Examples of the kind of timber engineering structural detail studied are shown in Figure 1. The purpose of this kind of detail is to provide a support area or an attachment point. In Swedish they are commonly called "knapar" or sometimes "upplagskonsoler" and in English they can be called cleats, studs or support consoles. The kind of cleats studied is in simple terms a piece of wood glued to a glulam structural member and used to get across loads from beams, bars and cables to a beam or a column. The cleats are often both glued and screwed to the beam or column, but the purpose of the screws is commonly just to give pressure and fixing while the glue hardens.

The alternative to using wooden cleats is to use some kind of metal device. Is has been argued that glued wooden cleats have the advantages of being cheaper and easier to handle, and perhaps also having a more attractive appearance. A disadvantage is that established method for strength design calculation seems to be lacking.

The purpose of the present experimental study is to contribute to knowledge for good strength design of glued wooden cleats. The tests are limited to cleats with its grain direction parallel with the grain direction of the actual structural member. The types of loading tested are limited to loads that don’t give rolling shear stress. The loading force vector is thus located within the plane created by the grain direction and the normal to the bond surface. The tests comprise a total of 19 testing series with a total of 75 individual cleat tests.

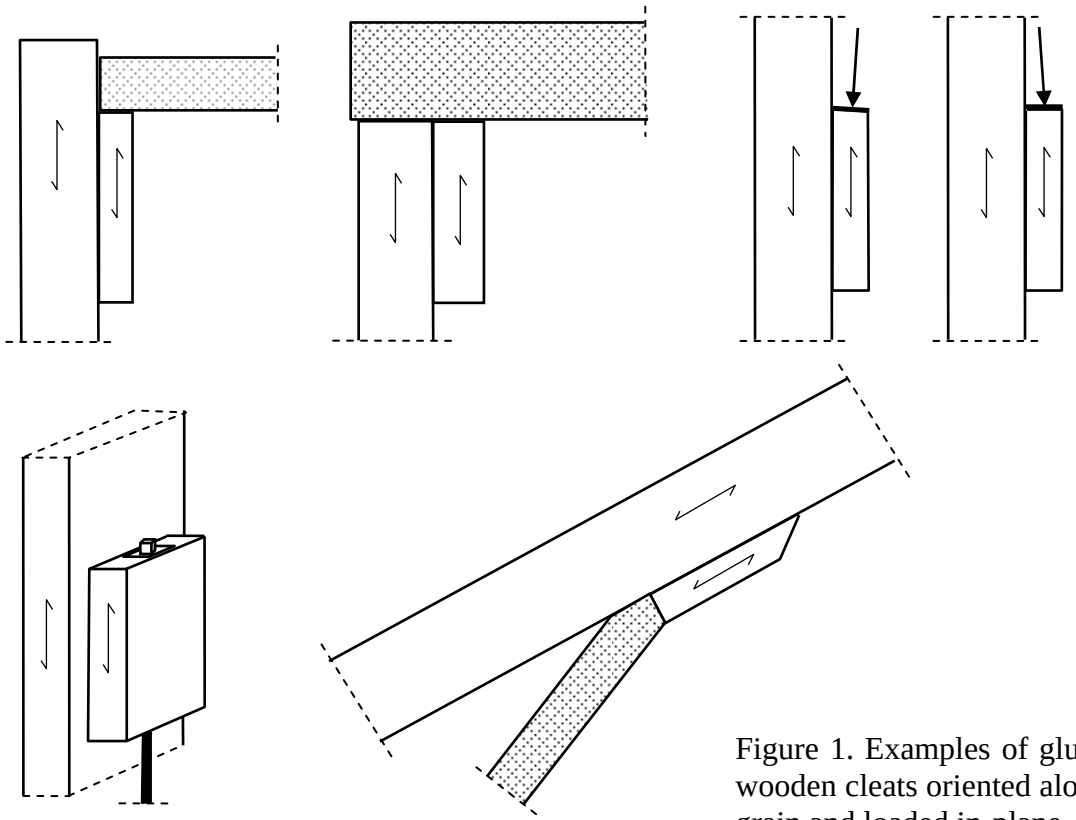

Figure 1. Examples of glued wooden cleats oriented along grain and loaded in-plane.

2. Specimens, setups, material, moisture conditions

2.1 Test series, specimen geometry and test setups

The testing comprised 16 basic test series and 3 completing test series. The 16 basic test series are denoted a, b, c … …, o and p. The 3 completing test series are denoted q, r and s. Series b serves as reference for several of the other tests and comprised 6 nominally equal tests. The other basic series comprised 4 nominally equal tests each, and the completing series 3 nominally equal tests each. The purpose of each test series is indicated in Table 1. Specimen geometry and type of load and support conditions are shown in Figures 2-8. The thickness of the cleat and the column was in all cases 115 mm.

Table 1. Purpose of cleat strength testing series

Series	Purpose of tests	Figure
a, b, c, d, e, f, g	Influence of size and shaping of cleat and column	2
h, i	Influence of screws	3
j, k	Influence of load inclination and orientation	4
l, m	Influence of cleat location at top of column	5
n	Influence of cleat placing at wide-side of column	6
o, p	Influence of climate variation	7
q, r, s	Verification of influence of load inclination	8

The locations of the supports are for all series such that the global line of force action through the structural member is either vertical or inclined 6.3^o relative to a vertical axis. If the roller supports act like ideal roller supports, then the force acting across the cleat bond area is a pure shear force for all test series with exception only for series k and r.

The load was for all series but k applied by vertical upward movement of an actuator on which the lower fixed support was placed. All these test were made by means of a sturdy 10 MN testing machine for loading and attachment of the supports. The machine can be seen in the pictures in Section 2.4. For series k was steel bars of the lower support attached to a vertically moving pulling actuator. These tests were made by means of a modern 500 kN MTS testing machine. The rate of the actuator movement was throughout 2 mm/min and the time to failure in order of 2-5 minutes.

The test setups and the support arrangements are shown in Figures 9-11. For all series but series j, l, m, r and s there are one horizontal and one vertical roller support at the top of the specimen. For series j, l, m, r and s there is a fixed support at the top. For series l, m and r this was realized by use of the same welded steel box support arrangement as in the other tests, see right hand side of Figure 9, and in series j and s by use of a vertical cylindrical steel console screwed to the testing machine, see right hand side of Figure 11.

The load cell used to measure the load is placed under the specimen and is oriented according to the line of force action, i.e. either vertical or with a 6.3^o inclination. The vertical component of a recorded load P is 0.994 P when the inclination is 6.3^o. The

bump-shaped contact surface of the load cell to the steel plate at the lower end of the wood constitutes the lower fixed support. The load acting on the load cell due to the dead weight of the specimen is not included in the recorded loads.

The force acting on the cleat was by proper placing of a bump-shaped steel part in all cases located at the center of the upper surface of the cleat. The upper roller support that carries a horizontal force was placed 46, 125 or 250 mm above the cleat so that the ratio between nominal shear stress and nominal bending stress in the column at the level of the cleat became the same for all tests where a roller support carrying horizontal force was used.

The load, the actuator movement and the deformation across the cleat glue line were recorded during the course of each test. The deformation was measured with a pair of LVDT-gauges as will be discussed further in Section 3.3.

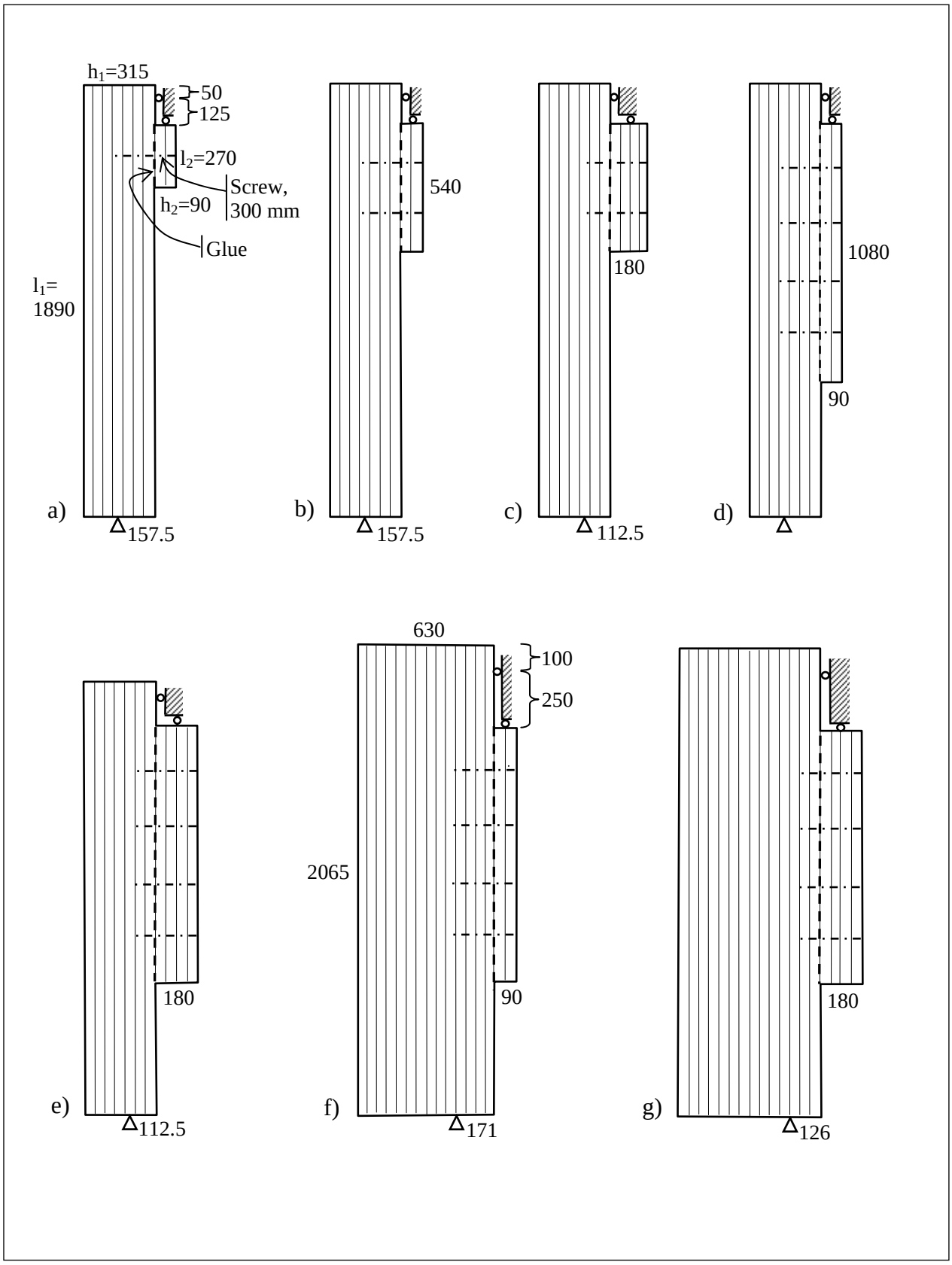

Figure 2. Test series a-g.

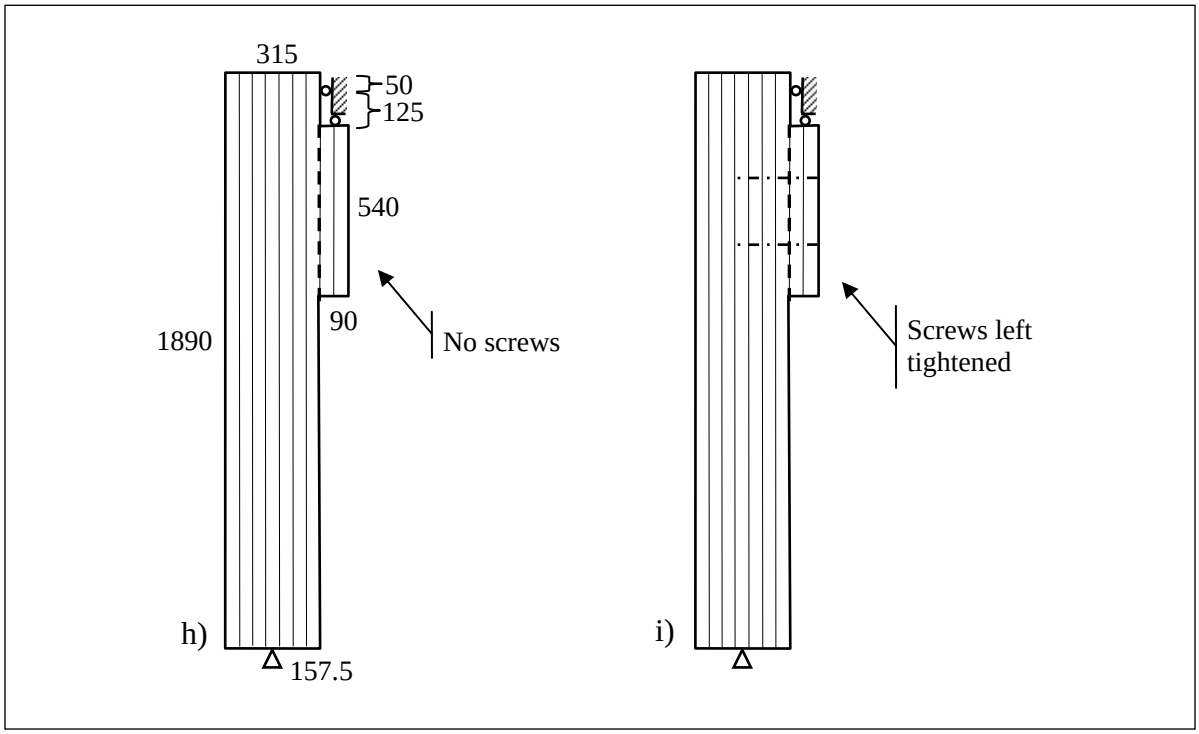

Figure 3. Test series h and i.

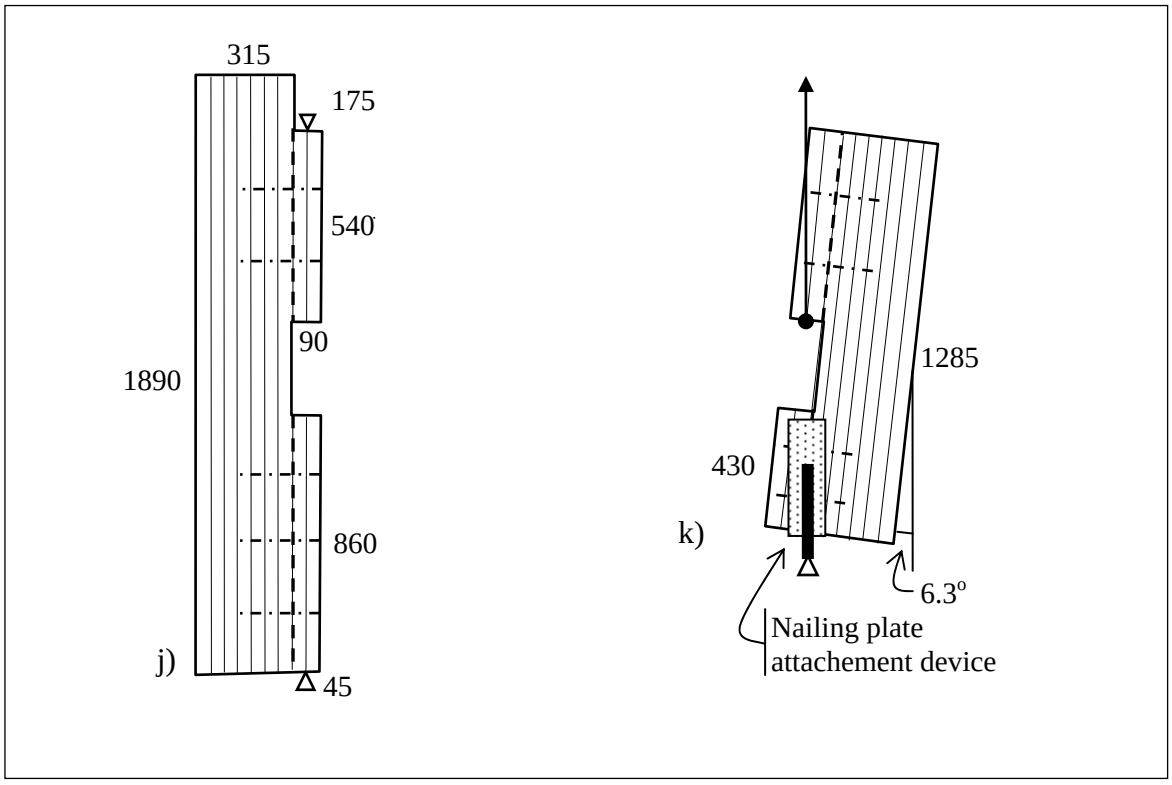

Figure 4. Test series j and k.

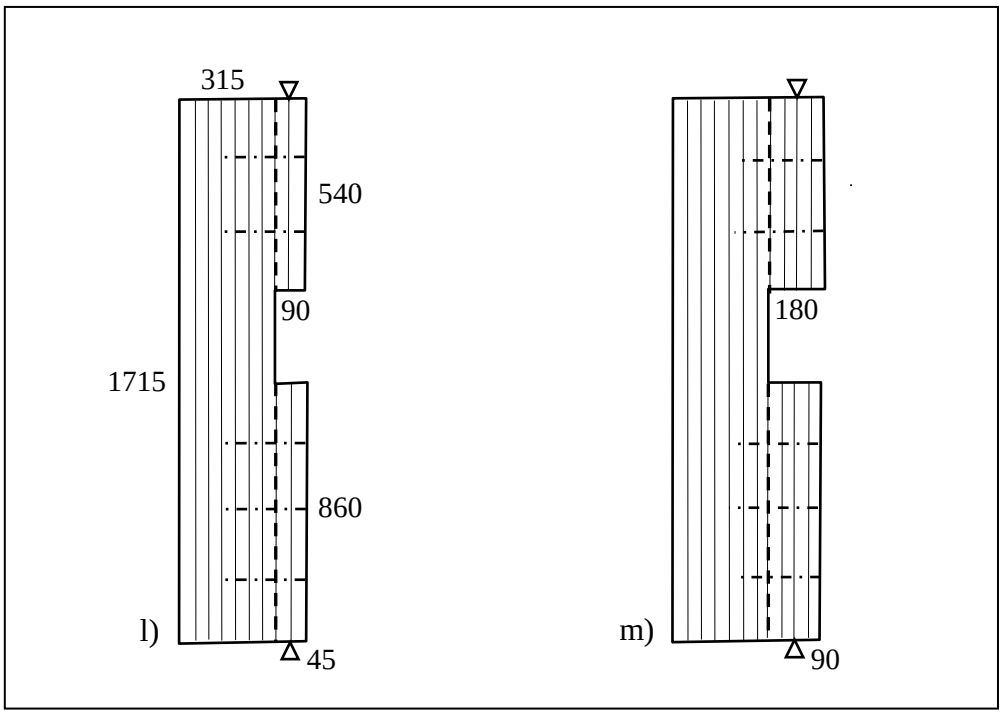

Figure 5. Test series l and m.

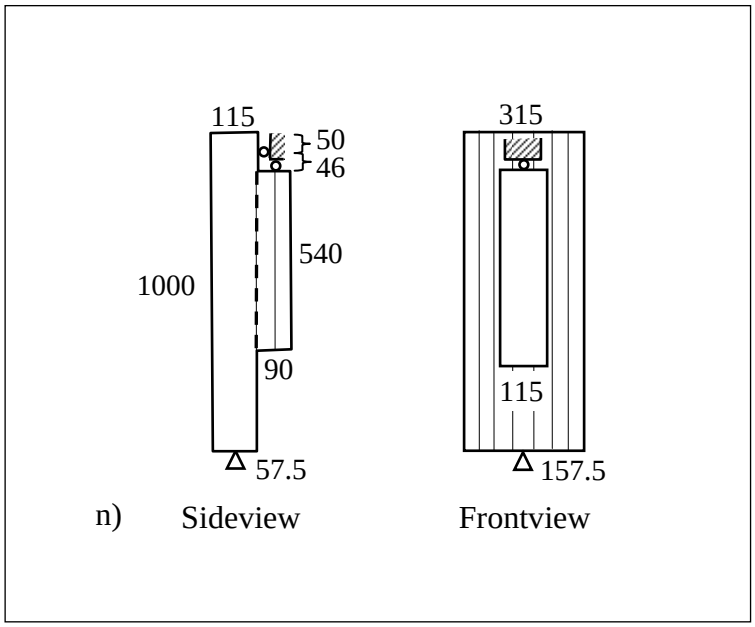

Figure 6. Test series n.

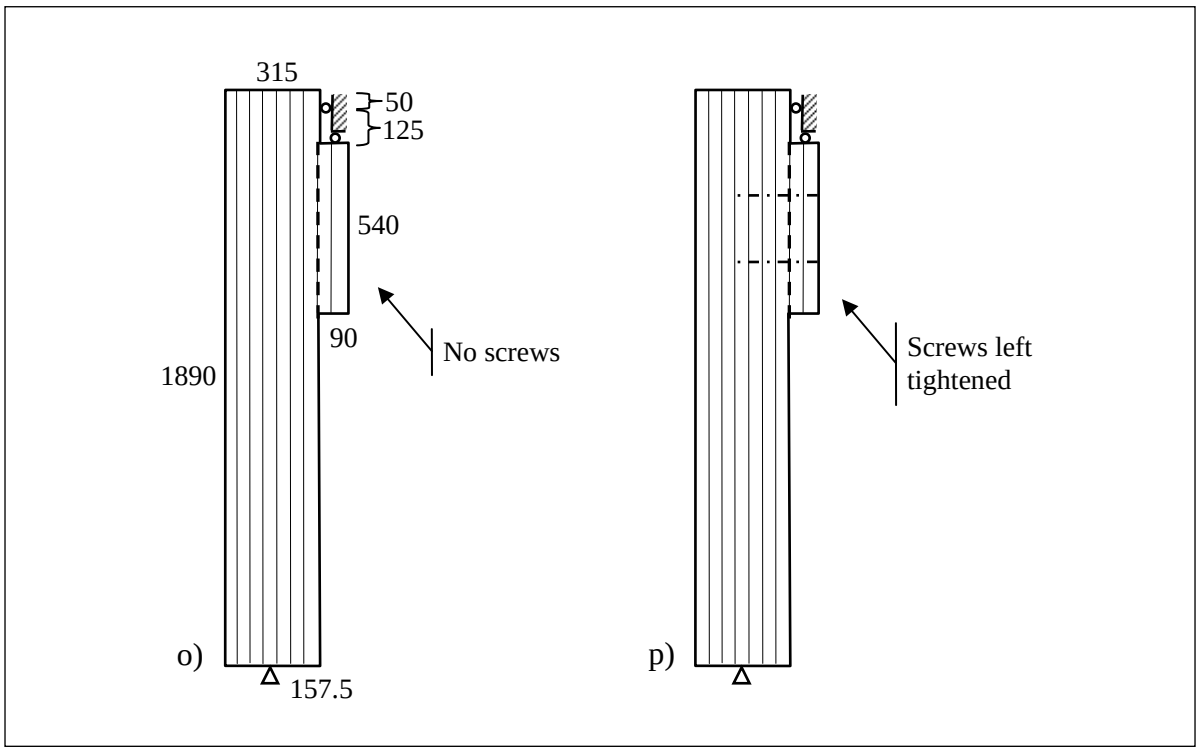

Figure 7. Test series o and p. Climate conditions indicated in Section 2.3.

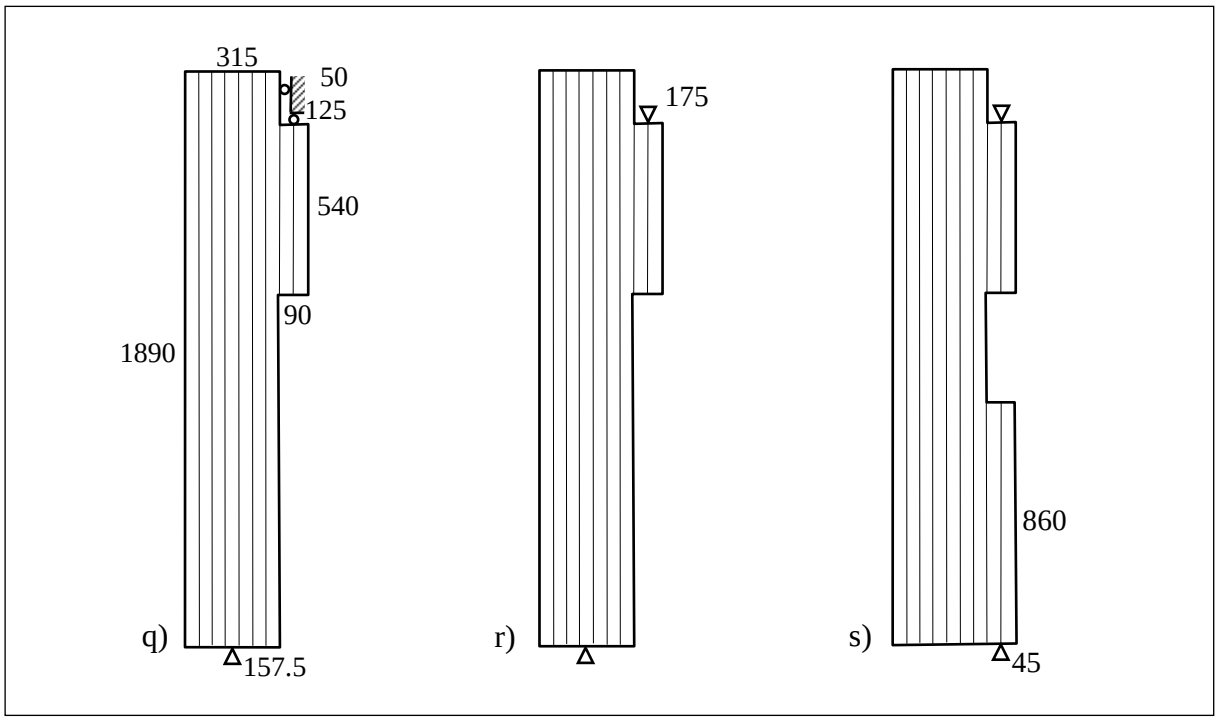

Figure 8. Test series q, r and s. These specimens were made of solid glulam, i.e. cut in one piece from a larger piece of glulam.

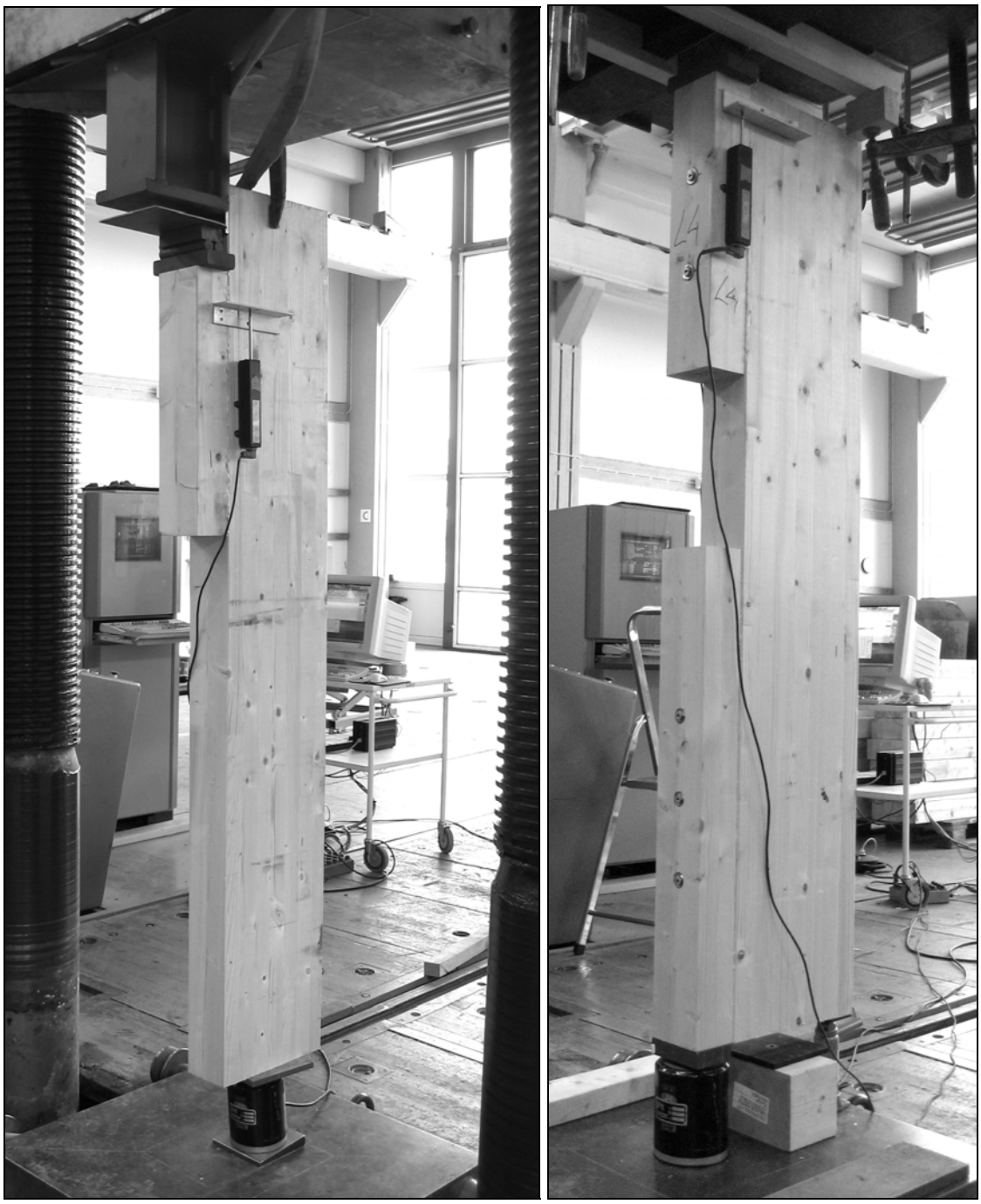

Figure 9. Test setup for test series with inclined global line of force action (left) and vertical line of force action (right).

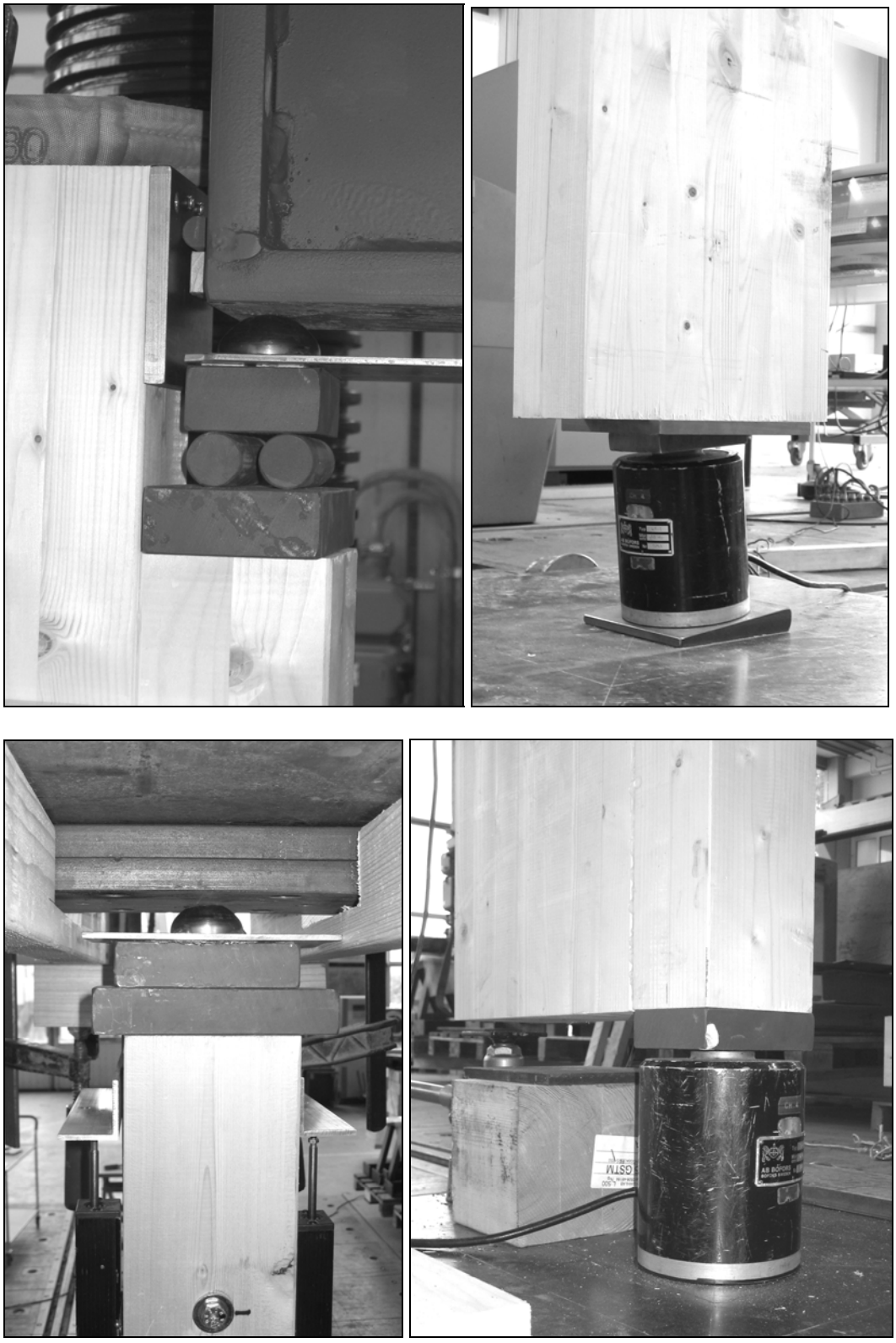

Figure 10. Support and load arrangements for series with inclined line of force action (upper) and for series with vertical line of force action (lower).

Figure 11. Test setup for test series k (left) and upper support in series j and s (right).

2.2 Material

2.2.1 Glulam

Manufacture of the glulam and gluing of the cleats were made in a glulam factory in Långshyttan, Sweden, owned by a member of Svenskt Limträ AB: Setra Trävaru AB. The glulam was made of spruce (Picea abies) and of quality L 40 with the same quality of the lamella in the entire beam cross section. The glulam glue was melamine. The beam thickness was 115 mm and the lamella thickness was 45 mm.

Density and moisture content was 443 kg/m^3 and 11.7 %, respectively, according to weighing of a few samples at the day of arrival to the testing laboratory, 2007-06-01. The average width of the growth rings was about 3.0 mm. The arrangement of the lamella with respect to the orientation of the annual rings is indicated in Figure 12. For the specimens in tests series q, r and s was the orientation varying according to the orientation of the larger pieces of glulam from which the test specimens were cut in one piece.

2.2.2 Screws

In most of the specimens there are screws, as indicated in Figures 2-8. The screws were placed so that the screw-to-screw distance and the screw to cleat end surface distance were the same. There is only one row of screws in each cleat. Taking series b as an example, there are 2 screws placed at a distance of 540/3=180 mm.

The screws used are shown in Figure 12. Their commercial term is SFS WFD-T, their length is 300 mm, the nominal diameter is 8 mm, the thread inclination is 4.5 mm/revolution and the measured diameter of the un-thread part of the screws is 7 mm. The diameter of the holes drilled for the screws through the cleats was 10 mm, which is slightly more the outer diameter of the threaded part of the screws. The diameter of the washer is 28 mm.

The screws were released, i.e. partly untied, before testing unless otherwise is indicated in the Figures 2-8. This release was to simulate the influence of possible drying and shrinkage of the wood. The release of the screws was 2/3 revolution for specimens with 90 mm cleats and 4/5 revolution for specimens with 180 mm cleats. This corresponds to 2.9 and 3.6 mm, respectively. This simulates 1.5 % shrinkage and was for screws of length 300 mm calculated according to: (90+210/2) x 1.5/100 = 2.9 mm and (180+120/2) x 1.5/100 = 3.6 mm.

2.2.3 Glue

The glue used to glue the cleats in series a-p was a two-component polyurethane, Purbond. The cleats were fixed during hardening of the glue either by the screws or, for the test specimens without any screws, by screw clamps.

The cleats in series q-s were not glued, the specimens were instead cut in one piece from larger pieces of glulam. The interface between the cleat part and the column part did, however, coincide with the location of a glue line in the glulam. The glulam glue was melamine.

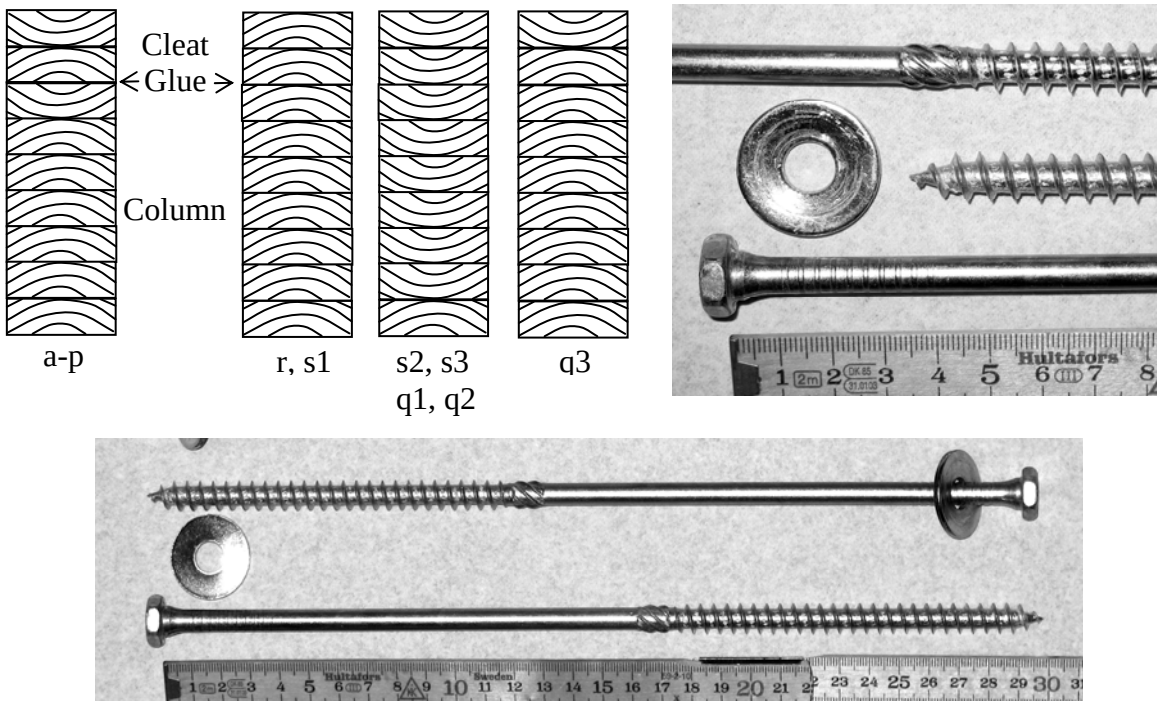

Figure 12. Orienting of lamella in specimens in series a-s (upper left), and screws.

2.2.4 Material for end-grain moisture sealing

The end-grain surfaces of the 8 specimens in series o and p were sealed before a wetting and drying treatment of these specimens. Mazonite high density fiber board of thickness 4 mm was nailed by anchorage nails and glued by a one-component polyurethane to the loaded end of the cleats. Aluminum foil was glued to all other end-grain surfaces of the specimens in series o and p, see Figure 14.

2.3 Moisture conditions, dates of testing and shrinkage

2.3.1 General

The glulam manufacture process makes is probable that the moisture content in the material was close to homogeneous at delivery. During the manufacture particular attention was made to equal moisture in the cleats and in the beams at the instant of gluing them together. According to weighing-drying-weighing of four samples of the approximate size 115x315x200 mm^3 was the mean moisture content 11.7 % at the day of delivery June 1, 2007.

2.3.2 Test series a-n and q-s

The specimens of series a-n were stored in the laboratory from the day of delivery to the day of testing. The dates of testing are indicated in Table 2 and the recorded climate in the laboratory is indicated in Figure 13. The relative humidity and temperature recordings are three hour mean values for 00.00-03.00, 03.00-06.00, etc. An example: the moisture value indicated for July at time 10.5 days is the mean value for the three hours from 09.00 to 12.00 of July 11. The specimens were placed in piles so that the end-surfaces, the 115 mm side edges and some of the beam side surfaces were exposed. Weighing of two specimens July 17 indicated a mean moisture content of 11.3 %.

The specimens tested February 13 2008 were cut February 11 from glulam left from series f and g. The specimens were stored in the laboratory from the day of delivery June 1 2007 to the day of testing. The mean RH and temperature in the laboratory during the period October 1 to February 13 was about 35-40% and 19^{o}C, respectively. Weighing and drying of two specimens February 13 indicated a mean moisture content of 9.7 %.

Table 2. Dates of strength testing, 2007 and 2008

Tests	Date	Tests	Date	Tests	Date	Tests	Date	Tests	Date
a	July 23	b4-6	Aug 28	k	Sept 12	o	Nov 5	q	Feb 13
b1-3	July 25-26	i	Aug 28-29	n	Sept 6	p	Nov 6	r	Feb 13
c	July 18-19	j	Aug 31					s	Feb 13
d	July 25	l	Aug 29-30						
e	July 19-20	m	Aug 31-3/9						
f	July 17-18								
g	July 16-17								
h	July 13								

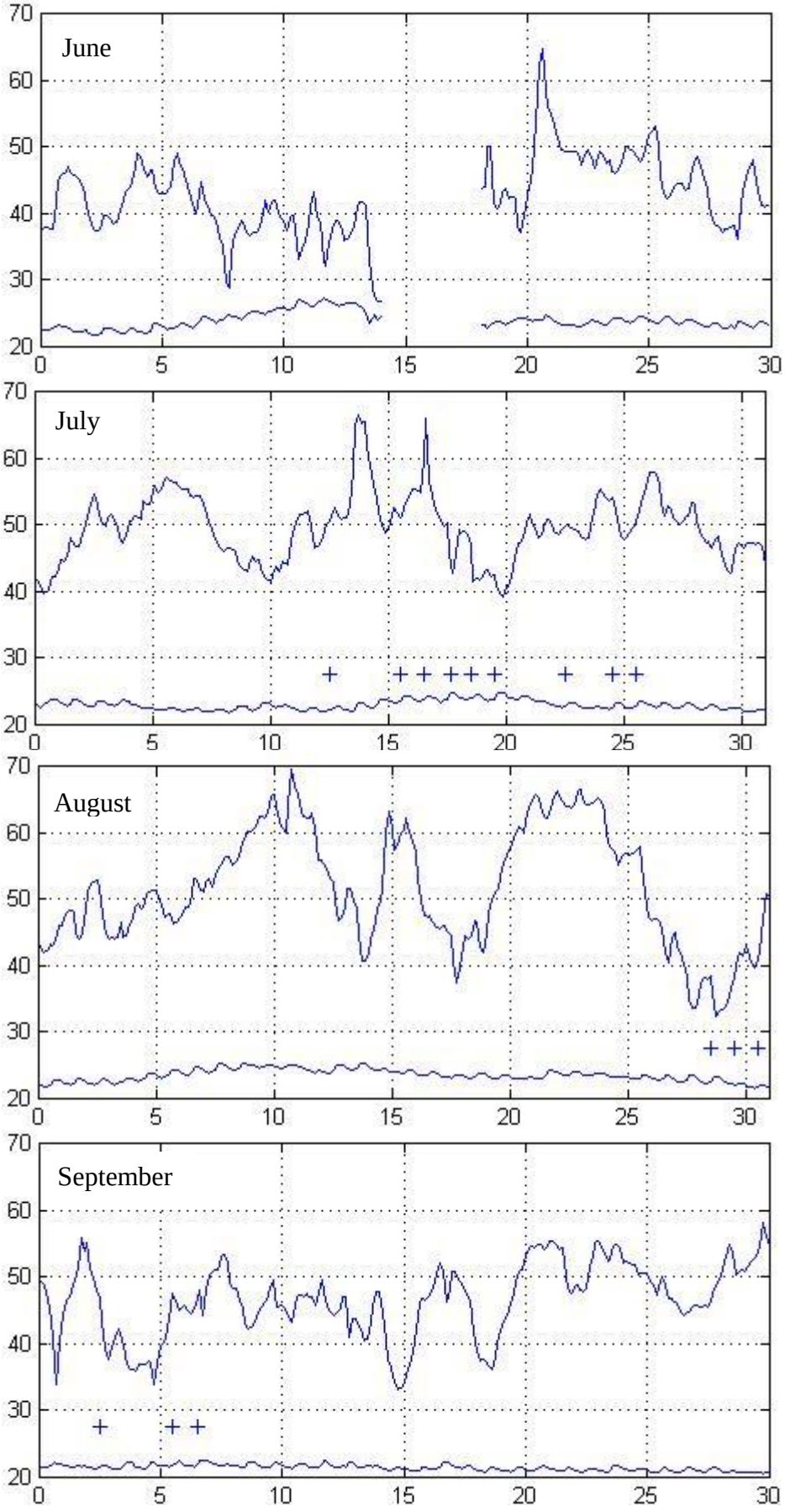

Figure 13. Relative humidity and temperature in laboratory. + indicates days of testing.

2.3.3 Test series o and p

The 8 specimens of series o and p were stored in the laboratory until June 26 and tested November 5 and 6. The specimens were in between these dates exposed to moisture conditions that roughly would simulate a possible exposure in practice: delivery of the material to a building site in late autumn, say in November or December, and exposed to a short rain at erection of the building. Then, for about two months, exposure to a high relative humidity, corresponding to a rain protected location without any heating in late autumn-winter. Then about 2.5 months in dry climates before the strength testing, the dry climates roughly corresponding to an in-door climate of a heated building during winter.

To simulate this moisture history, the specimens were first sprinkled with water for 20 minutes and then placed in climate chambers. Figure 14 shows the end grain surface moisture sealing of the specimens, lined up for sprinkling of water. The sealing is described in Section 2.2.

Table 3 shows the climatic conditions, the moisture content as determined by weighing of two of the specimens and the shrinkage during the periods of drying. The shrinkage was measured in a simple manner by use of a ruler. The lengths measured were the beam cross-section height of nominal dimension 315 mm and the corresponding measure 315+90=405 mm at the cleat. The moisture induced deformation was measured only during the drying periods. However, by comparison to length measures of other nominally equal specimens not exposed to the humid conditions, it seemed that the swelling during conditioning at 90 % RH was less than the subsequent shrinkage.

A kind of measure of shrinkage and creep was obtained also by tightening tests of a few screws: at the day of strength testing, the screws could be turned about 0.4 revolutions to be tightened, corresponding to about 0.4*4.5=1.8 mm play. The screws turned were turned back before the cleat strength testing.

Table 3. Series o and p: conditioning, mean moisture content and shrinkage.

Date	Time	RF	Temp.	MC	Change of 405 mm width	Change of 315 mm width
2007-06-01				11.70 %	-	-
	26 days	~ 43 %	~ 23 ^{o}C	- 0.39 %		
2007-06-26				11.31 %	-	-
	20 min.	"Rain"	~ 20^{o}C	+0 .61 %		
2007-06-26				11.92 %	-	-
	59 days	90 %	19.6^{o}C	+3.74 %		
2007-08-24				15.66 %	0.0 mm	0.0 mm
	28 days	42 %	23.3^{o}C	- 3.18 %	-3.1 mm	-2.4 mm
2007-09-21				12.48 %	-3.1 mm	-2.4 mm
	45 days	27 %	22.9^{o}C	- 1.64 %	-1.3 mm	-0.8 mm
2007-11-05				10.84 %	-4.4 mm	-3.2 mm

Figure14. End grain sealing of specimens in series o and p.

2.4 Testing site pictures

3. Test results

3.1 Failure loads

The failure loads recorded are indicated in Table 4 and Figure 15. The mean failure loads are indicated also in Table 5 together with short characterization of the different series. The loads indicated, P_f, are the maximum loads recorded by the load cell in the direction of the load cell, with the load set to zero when only the dead weight of the specimen was carried by the cell. h_1 and h_2 indicate the cross section height of the beam and the cleat, respectively, and l_2 the length of the cleat. The widths are $b_1=b_2=115$ mm, except for series n where $b_1=315$ mm.

The error bars shown in Figure 15 indicate 90 % confidence intervals for the mean values. This means that there is a 90 % probability that the mean value found would be within this interval if an infinite number of nominally equal test were made. The interval was calculated for a normal distribution with unknown value of the true standard deviation: $I = \bar{P}_f \pm t_\alpha(\alpha/2, n-1)\, s/\sqrt{n}$ where the bar indicates mean value, s the standard deviation of the sample tested, n the number of tests and where the numerical values for the t_α-distribution can be found in mathematical tables. For n=4 and $1-\alpha=0.90$ is $t_\alpha=2.35$.

The compiled coefficient of variation for all tests is 11.8%. This value is calculated as the square rote of the mean of the coefficient of variation in square for the test series, taking into account the different numbers of tests in the different series.

Table 4. Recorded loads at failure, P_f.

Ser.	h_1 mm	l_2 mm	h_2 mm	Failure load, P_f, kN Test1	Test2	Test3	Test4	Test5	Test6	Mean P_f, kN	Cov, %
a	315	270	90	50.9	45.0	48.2	49.6	-	-	48.4	5
b	315	540	90	215.4	164.5	183.8	163.2	130.4	159.2	169.5	17
b1-3	315	540	90	215.4	164.5	183.8	-	-	-	187.9	13
b4-6	315	540	90	-	-	-	163.2	130.4	159.2	150.9	12
c	315	540	180	87.6	87.5	70.5	98.4	-	-	86.0	13
d	315	1080	90	283.7	256.3	229.0	237.5	-	-	251.6	10
e	315	1080	180	267.2	284.2	273.6	281.9	-	-	276.7	3
f	630	1080	90	269.4	331.5	240.1	260.4	-	-	275.3	14
g	630	1080	180	271.3	224.1	282.3	298.1	-	-	269.0	12
h	315	540	90	123.0	110.8	111.0	128.4	-	-	118.3	7
i	315	540	90	142.7	173.1	196.2	185.7	-	-	174.5	13
j	315	540	90	93.2	91.7	92.6	111.4	-	-	97.3	7
k	315	540	90	33.4	39.0	42.4	38.8	-	-	38.4	10
l	315	540	90	135.0	116.4	139.3	141.2	-	-	133.0	9
m	315	540	180	94.0	93.1	96.7	96.9	-	-	95.2	2
n	115	540	90	214.4	172.9	177.7	190.9	-	-	189.0	10
o	315	540	90	129.9	110.3	120.9	109.8	-	-	117.8	8
p	315	540	90	109.5	150.4	165.3	91.1	-	-	129.1	27
q	315	540	90	141.1	105.0	134.9	-	-	-	127.0	15
r	315	540	90	240.0	229.6	249.3	-	-	-	239.6	4
s	315	540	90	103.4	100.7	98.8	-	-	-	101.0	4

Figure 15 and Table 5. Recorded failure loads, P_f, in kN.

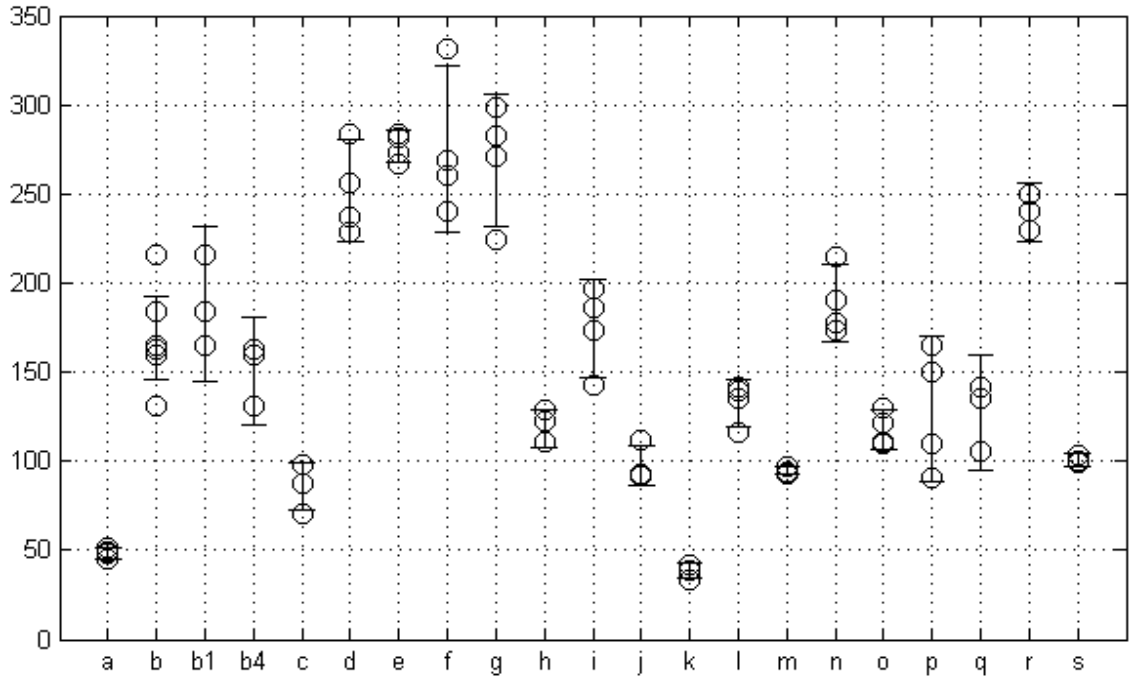

Ser.	h_1 mm	l_2 mm	h_2 mm	Remark	Mean P_f kN	Mean $P_f/(l_2 b_2)$ MPa
a	315	270	90	Shorter cleat	48	1.56
b	315	540	90	Reference case	169	2.73
b1-3	315	540	90	Specimens in b-series tested July 25	188	3.03
b4-6	315	540	90	Specimens in b-series tested Aug. 28	151	2.43
c	315	540	180	Thicker cleat	86	1.43
d	315	1080	90	Longer cleat	252	2.03
e	315	1080	180	Longer thicker cleat	277	2.23
f	630	1080	90	Longer cleat on larger beam	275	2.22
g	630	1080	180	Longer thicker cleat on larger beam	269	2.17
h	315	540	90	No screws	118	1.91
i	315	540	90	Screws not untied	174	2.81
j	315	540	90	Vertical load	97	1.57
k	315	540	90	Tensile load comp. Beam in tension	38	0.62
l	315	540	90	Cleat at top of beam. Vertical load	133	2.14
m	315	540	180	Thicker cleat at top. Vertical load	95	1.53
n	115	540	90	Cleat placed on beam side	189	3.04
o	315	540	90	Wetting-drying. No screws	118	1.90
p	315	540	90	Wetting-drying. With screws	129	2.08
q	315	540	90	Solid glulam	127	2.05
r	315	540	90	Solid glulam. Compr. load comp.	240	3.86
s	315	540	90	Solid glulam. Vertical load	101	1.63

3.2 Locations and pictures of fracture

The locations of fracture can be seen in the pictures in the below 8 pages, presented without any figure captions. For each test series two pictures are shown: in most cases the left and the right hand side of one specimen. The failures shown are estimated to be the most typical for each series. No obvious difference in location and type of failure was observed for the different series with the exception for series l and m.

With the exception of series l and m, failure started at the upper corner of the cleat. In most cases failure was initiated in the wood very close to the bond line and then propagated in the wood of the beam or the cleat, roughly along the glued area and probably according to the orientation of the grain in the wood.

The initiation of the fracture seemed for some specimens partly to take place in the glue line, probably in the interface between the wood and the glue. Also in almost all of these cases, the subsequent fracture propagation took place within the wood, outside the actual glue surface. Figures 16 and 17 show pictures of fracture surfaces, estimated to be typical for the fractures observed.

Series l and m related to placing of the cleat as a console at the top of the column. In most of these tests failure took place as a perpendicular to grain tensile failure in the top of the column, see below pictures showing specimens from series l and m. The location of the fracture surface is indicated in Table 6 as the approximate horizontal distance from the cleat bond area to the failure surface at the top of the column.

Table 6. Location of fracture for series l and m.

Series l (h_2=90 mm)		Series m (h_2=180 mm)	
Specimen	Distance, mm	Specimen	Distance, mm
l1	102	m1	1
l2	88	m2	64
l3	90	m3	96
l4	79	m4	0
Mean	90	Means	80 and 0.5

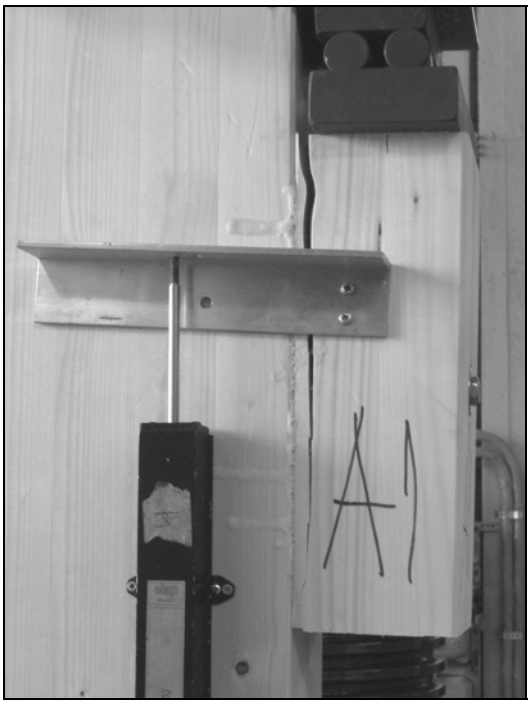
A1


A1
30
CH 3


B1


B1

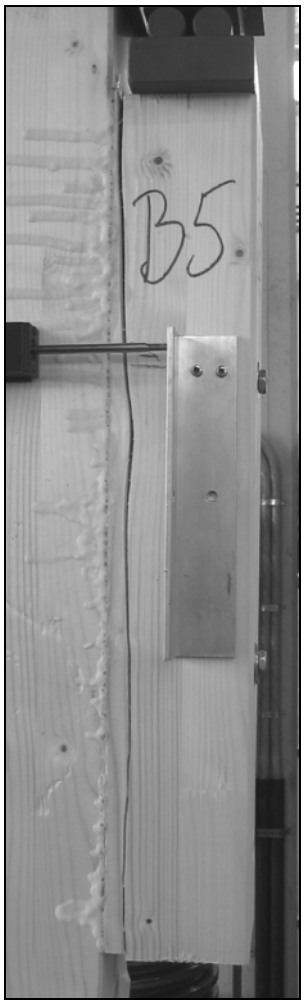
B5

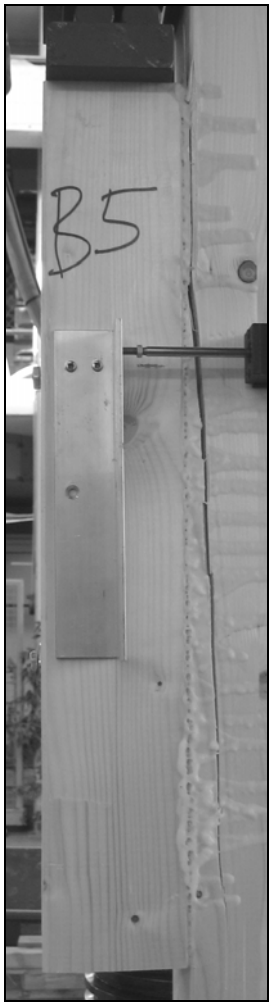
B5


C1

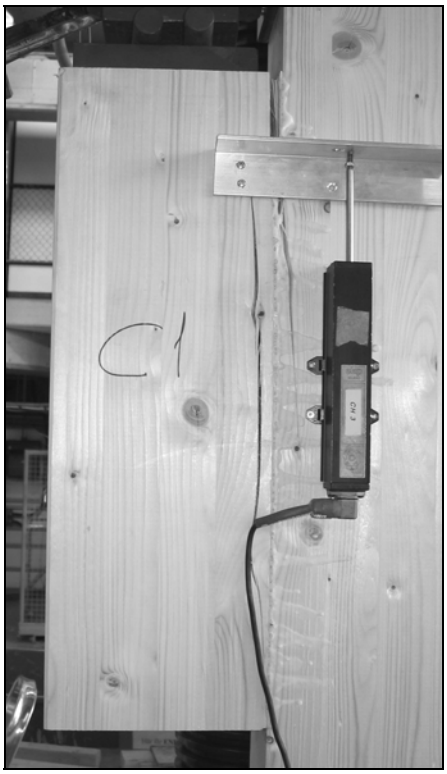
C1

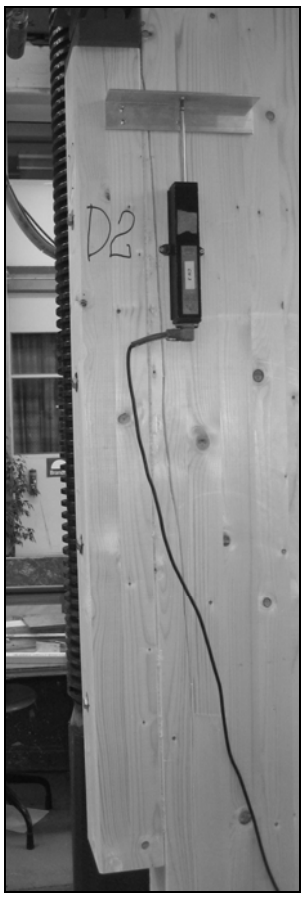
D2


D2


E4


E4


F3
F3
G1
G1


43
43
I1
I1


J2


J2


K3


K3


L3


L4


M2

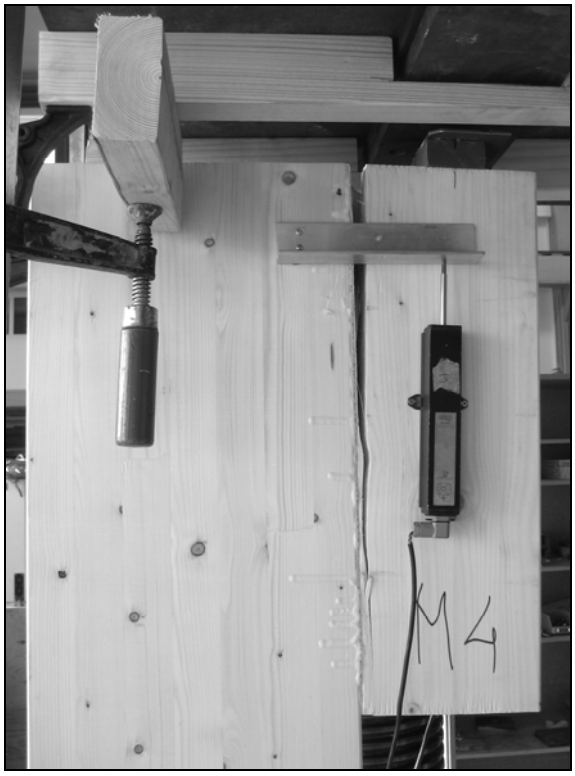
M4


M1

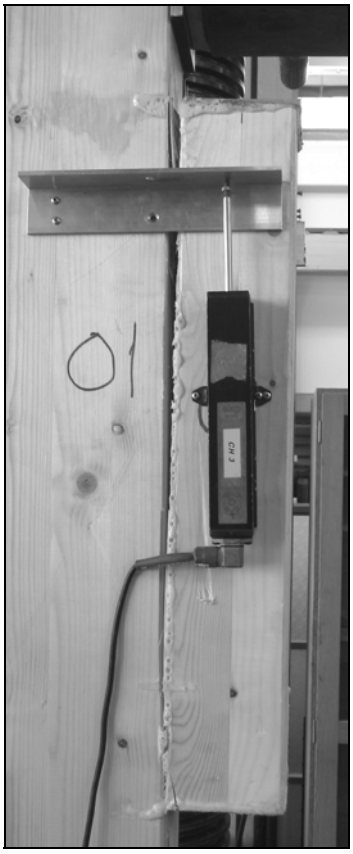
01


01


02


P1


P2


P4

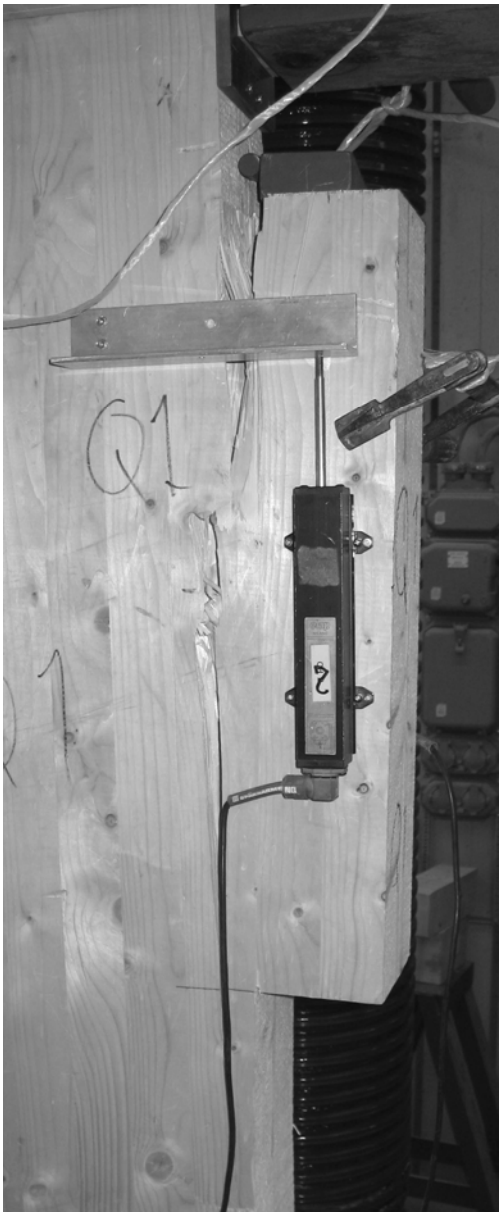
Q1


Q2
Q2
Q2
Q2


R1

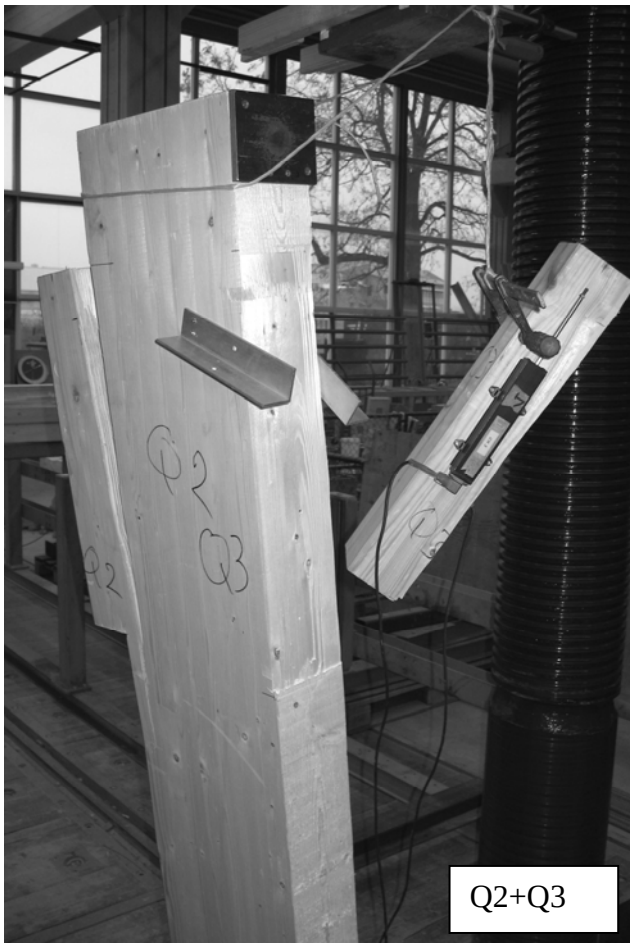
Q2
Q3
Q2+Q3


R2


S2
S3

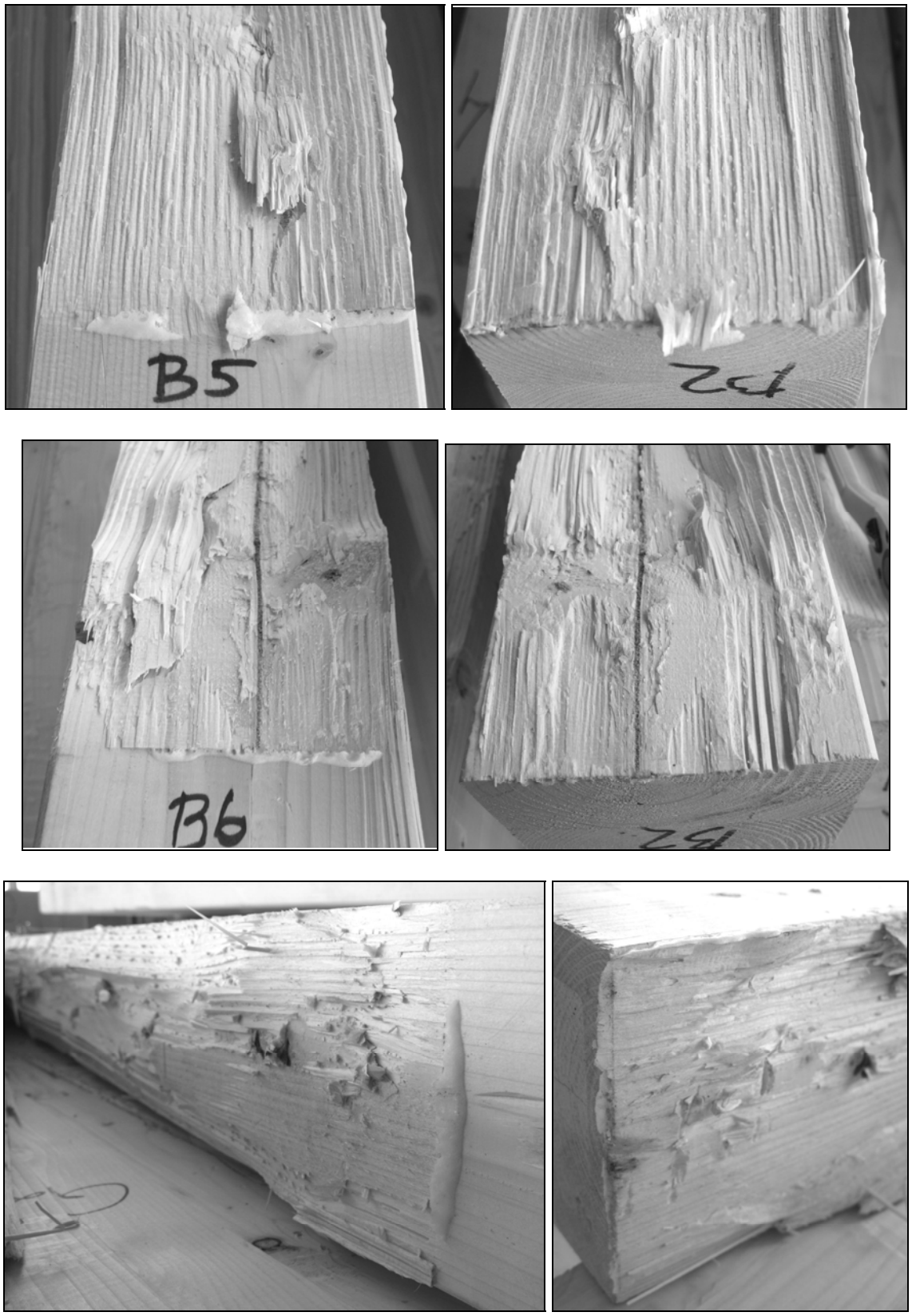

Figure 16. Beam side (left) and cleat side (right) of specimens b5, b6 and g1.

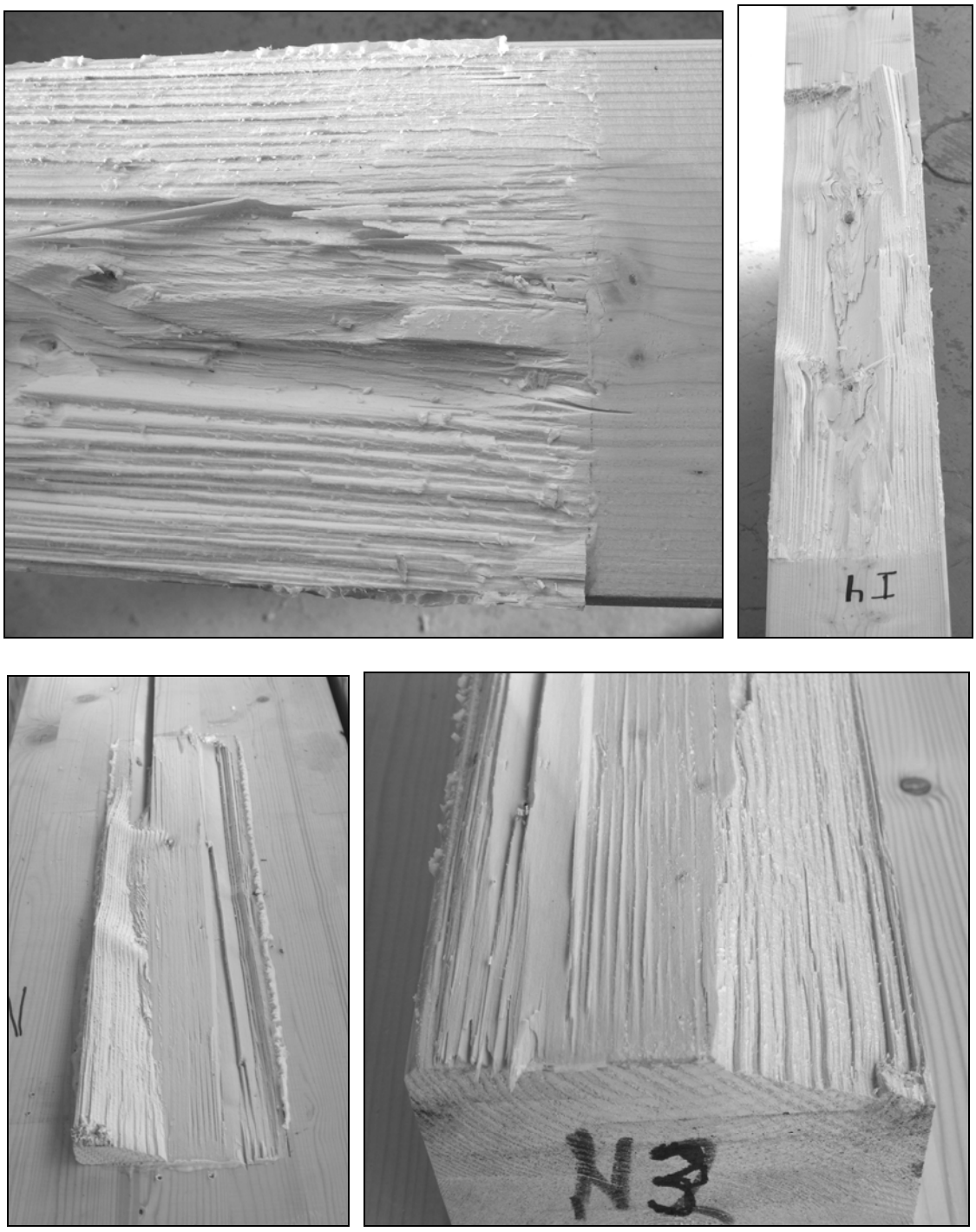

Figure 17. Beam side of specimen i4 (upper left and right) and beam side (lower left) and cleat side (lower right) of n3.

3.3 Load versus measures of deformation

The load was recorded versus the movement of the actuator of the testing machine and versus a deformation measured by a pair of LVDT-gauges. The actuator movement corresponds to the total deformation, including the deformation of the specimen and also the deformations in the support arrangements, the load cell and the testing machine itself.

The two LVDT-gauges were placed one at each side of the specimen as can be seen in Figure 9 and in several pictures in Section 3.2, for instance the picture showing specimens a1 and c1. The gauges were orientated vertically in all tests with the exception only for the three test b4-6. The gauges were in those three tests oriented horizontally in order to measure opening of the crack. The LVDT was fixed to the column part or the cleat part of the specimen by means of two screws. The bar of the gauge rested against at small horizontally oriented metal cantilever fixed by two screws to the opposite part of the specimen. This means, for the case of location of the LVDT at the column part, that the recorded deformation is the relative vertical movement between the column side and the cleat side plus the rotation of the cleat side times the length of the cantilever. A positive value of the deformation corresponds to elongation. As an example, if shear slide along the cleat bond line was the only deformation, then a negative deformation would be recorded. In the case of location of the LVDT at the cleat, it is the opposite.

Figure 18 shows for each test series the mean curve for load versus displacement, i.e. versus actuator movement. The mean curves were determined by normalizing the individual curves with respect to mean load and displacement at peak load, and then calculating the average normalized load for a large number of normalized displacements before finally multiplying normalized load and displacement with the mean absolute load and displacement at the peak point.

On the following 5 pages are 38 diagrams that show the recordings for the individual tests. The left hand side of the pages shows the load in kN versus the actuator movement in mm and on the right hand side they show the load versus the LVDT-recording in mm. The LVDT measure shown is the mean of the values given by the left and the right gauge. The placing of the LVDT gauges was somewhat different for the different test series as can be seen in the pictures in Section 3.2. The LVDT-recordings are shown only up to the instant of maximum load. Any meaningful LVDT recordings were commonly not possible after the commonly very brittle failure events at peak load.

The curves for load versus LVDT-recording show in general a non-linear performance corresponding to predominant shear deformation along the glue line region at the lower loads and predominant cleat rotation reflecting start of crack opening at loads closer to the ultimate failure load.

The diagrams for load versus total deformation, i.e. versus the actuator movement, shows a slight decrease in stiffness in a loading range from about 80 to about 100 kN. This magnitude of load is most probably corresponding to the weight of the cross-head of the testing machine. The force in the threading in the big screws that carry the cross head is thus changing direction at this load. This means that any small play or lack of pre-pressure in the screw to nut connection gives a decrease in total stiffness at the load corresponding to the weight of the head.

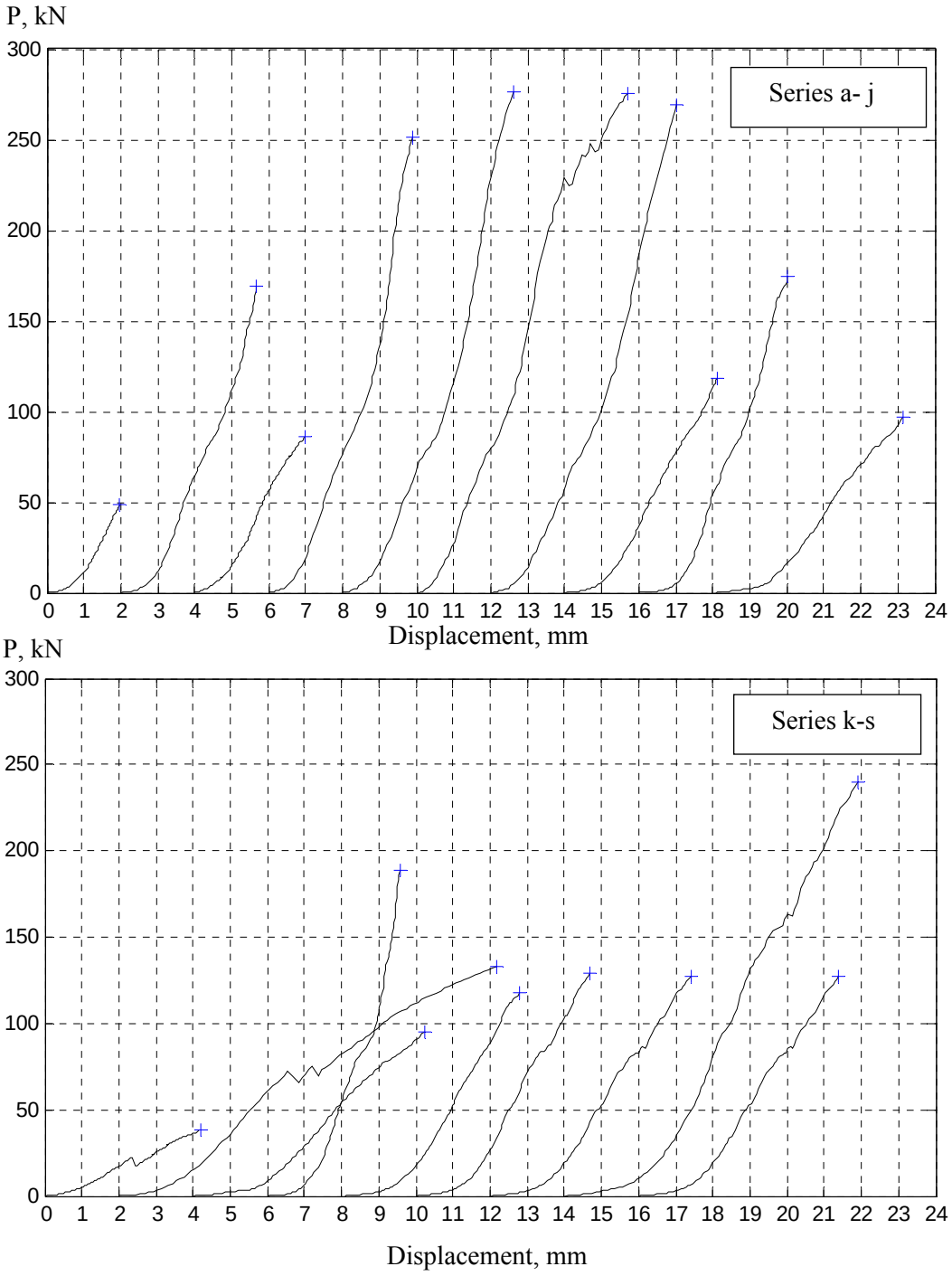

Figure 18. Mean curves for load versus displacement for series a-s. The curves are separated 2 mm.

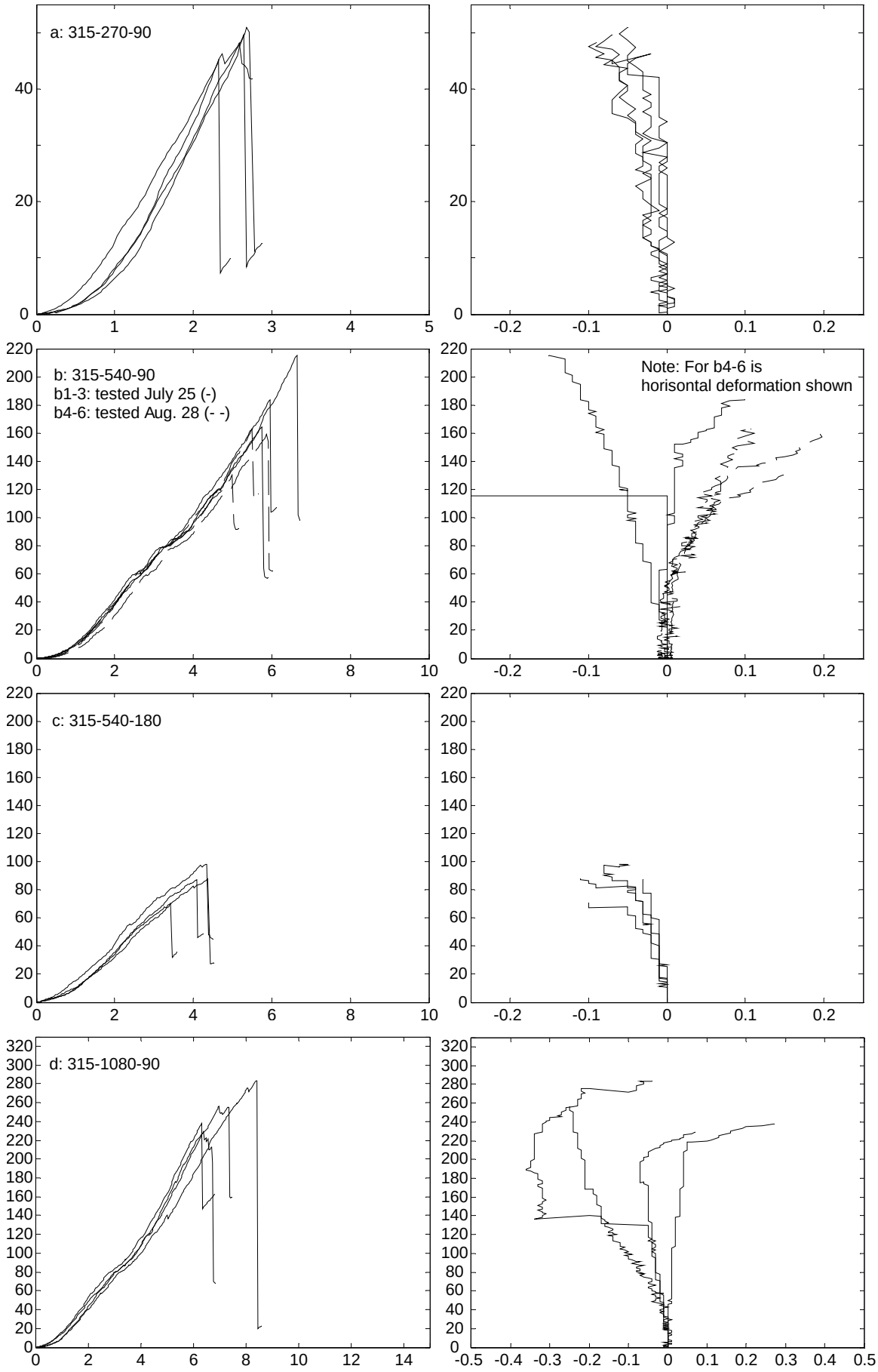
a: 315-270-90
b: 315-540-90
b1-3: tested July 25 (-)
b4-6: tested Aug. 28 (- -)
Note: For b4-6 is
horisontal deformation shown
c: 315-540-180
d: 315-1080-90

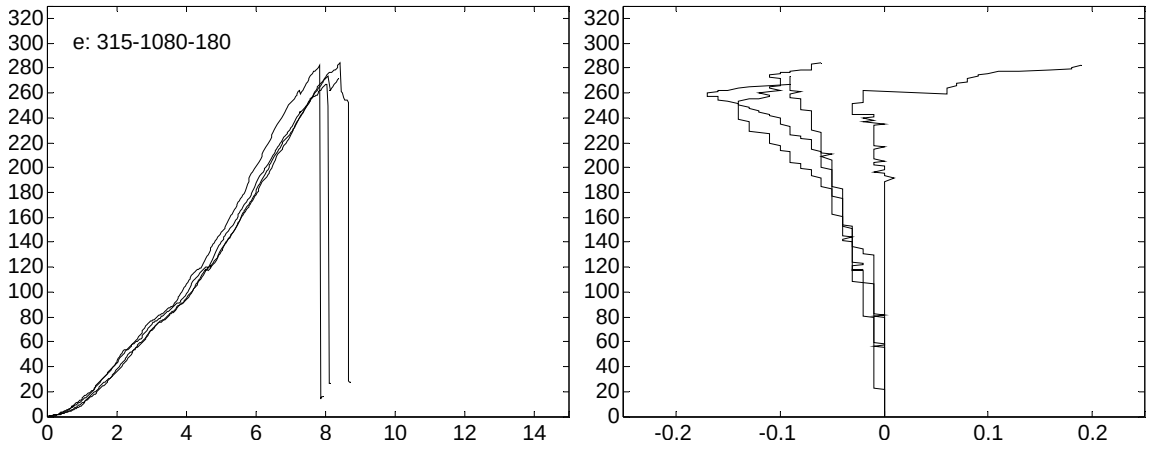
e: 315-1080-180

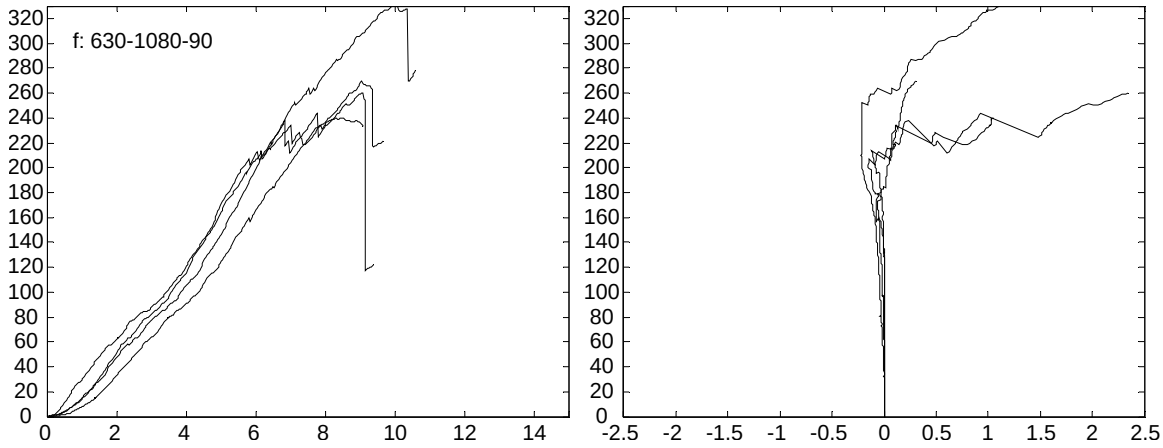
f: 630-1080-90

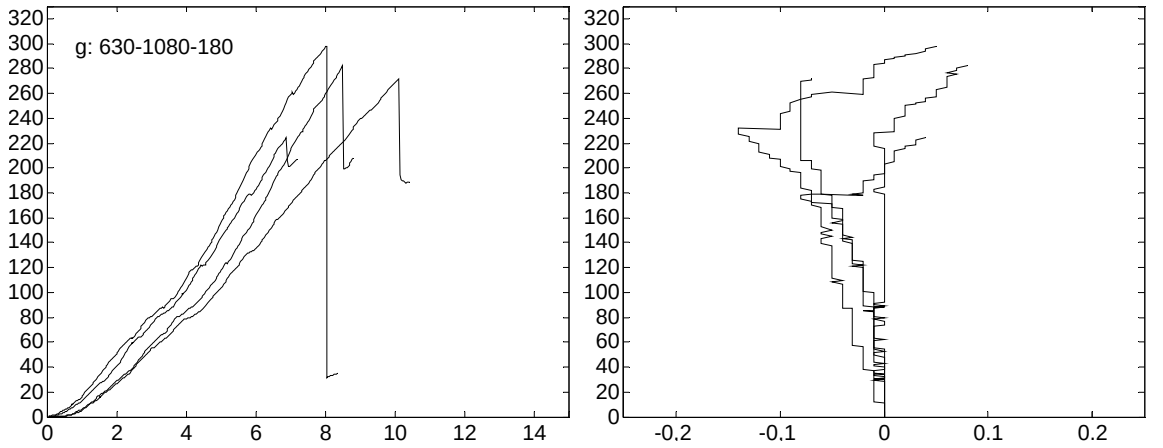
g: 630-1080-180

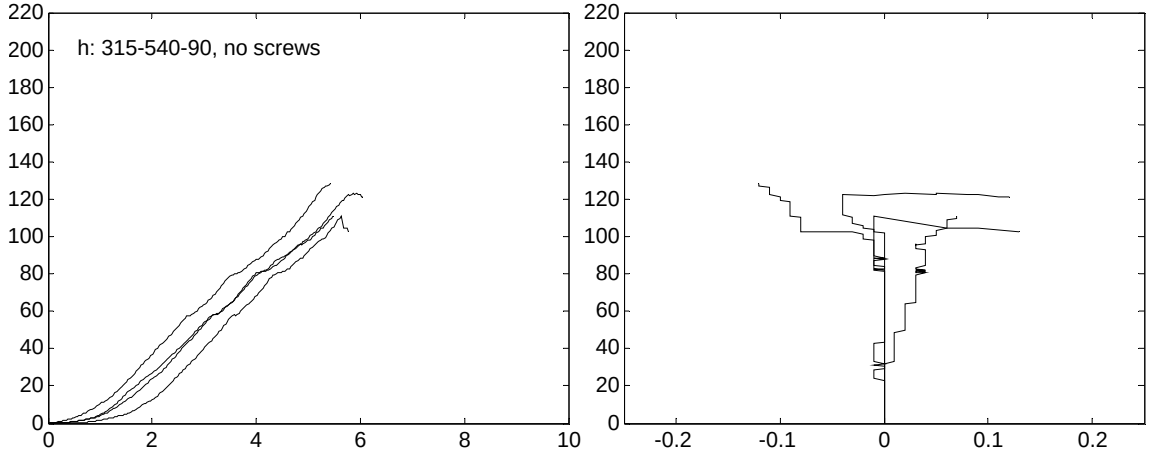
h: 315-540-90, no screws

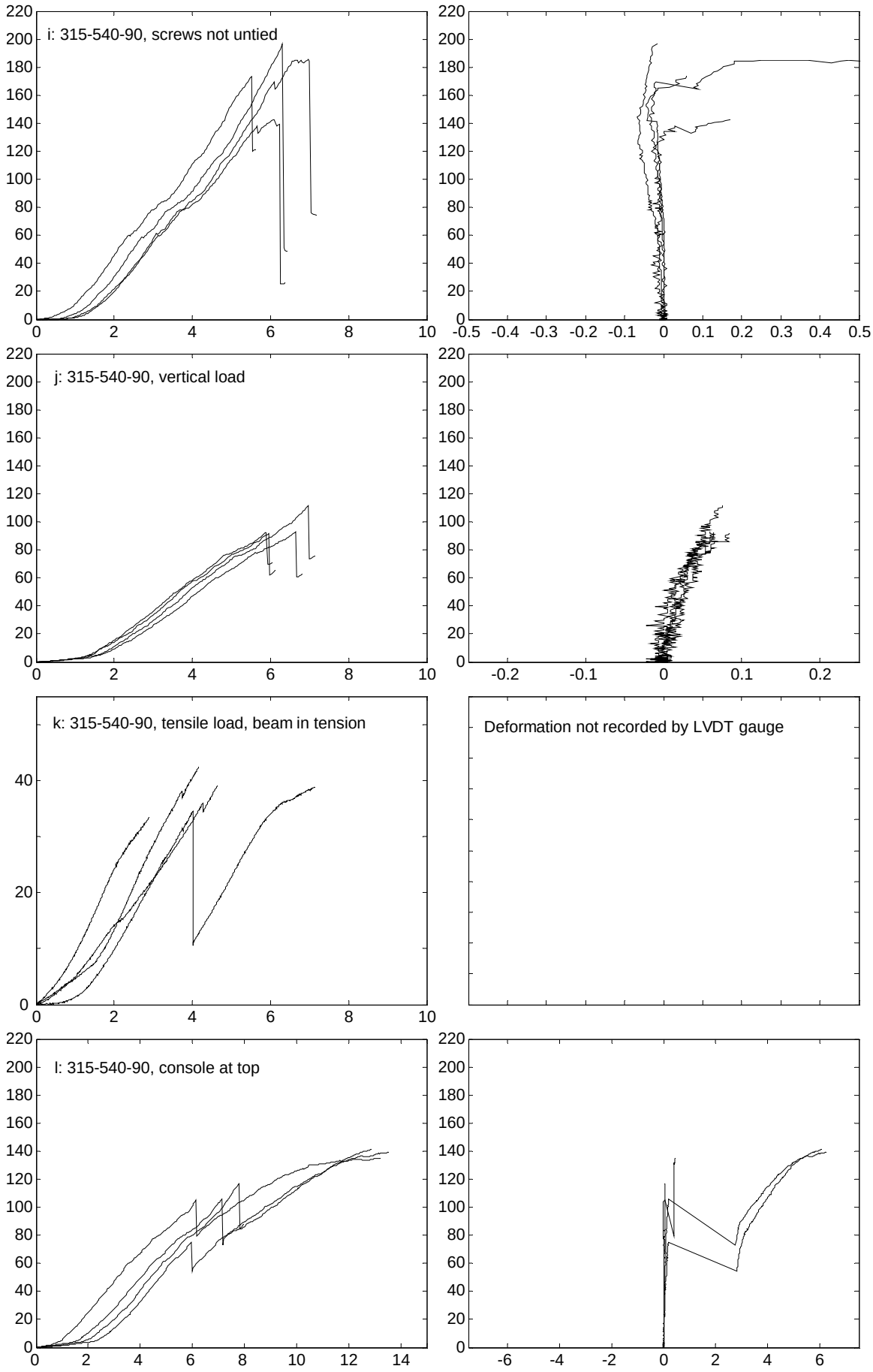
i: 315-540-90, screws not untied
j: 315-540-90, vertical load
k: 315-540-90, tensile load, beam in tension
Deformation not recorded by LVDT gauge
l: 315-540-90, console at top

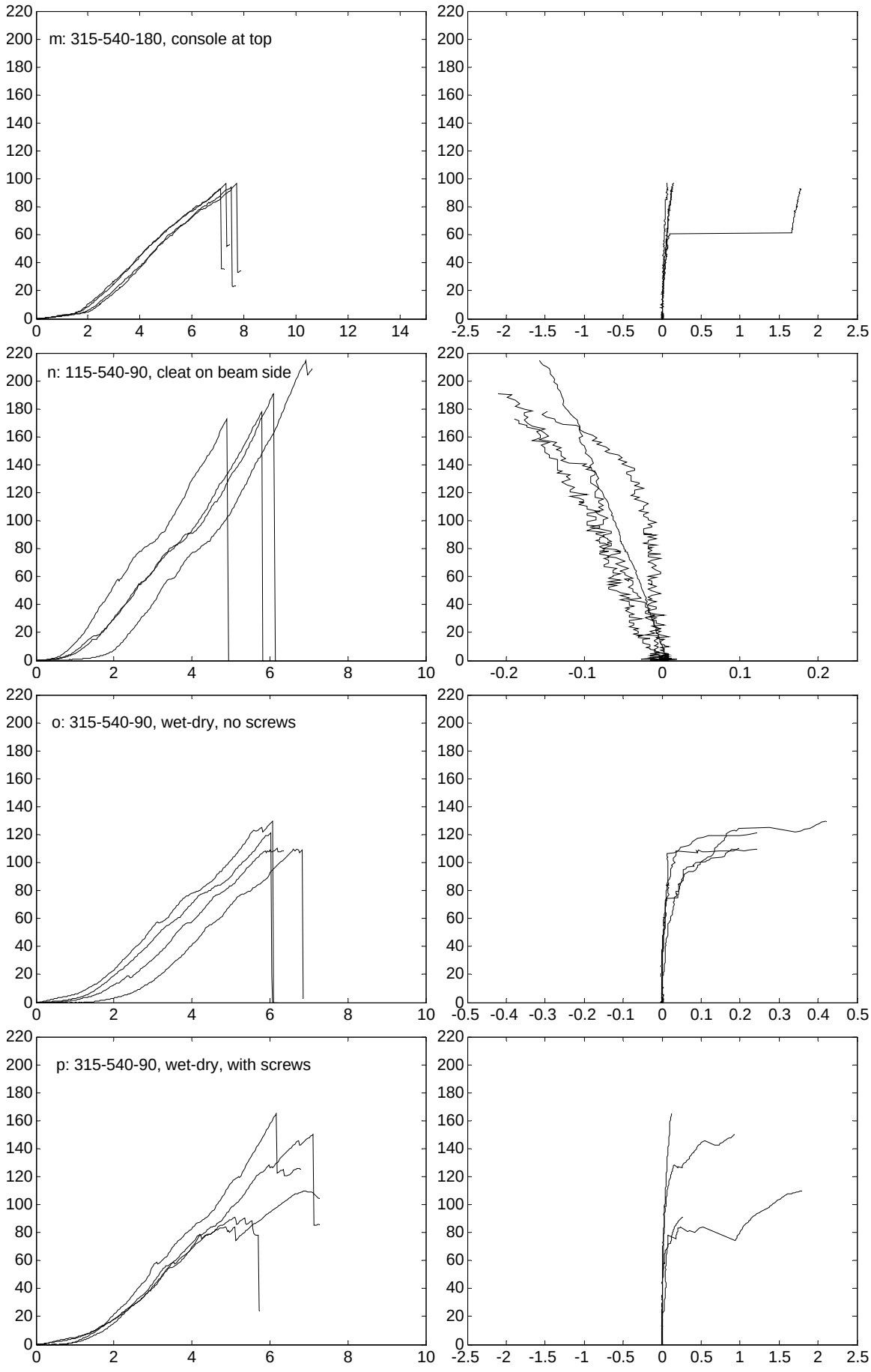
m: 315-540-180, console at top
n: 115-540-90, cleat on beam side
o: 315-540-90, wet-dry, no screws
p: 315-540-90, wet-dry, with screws

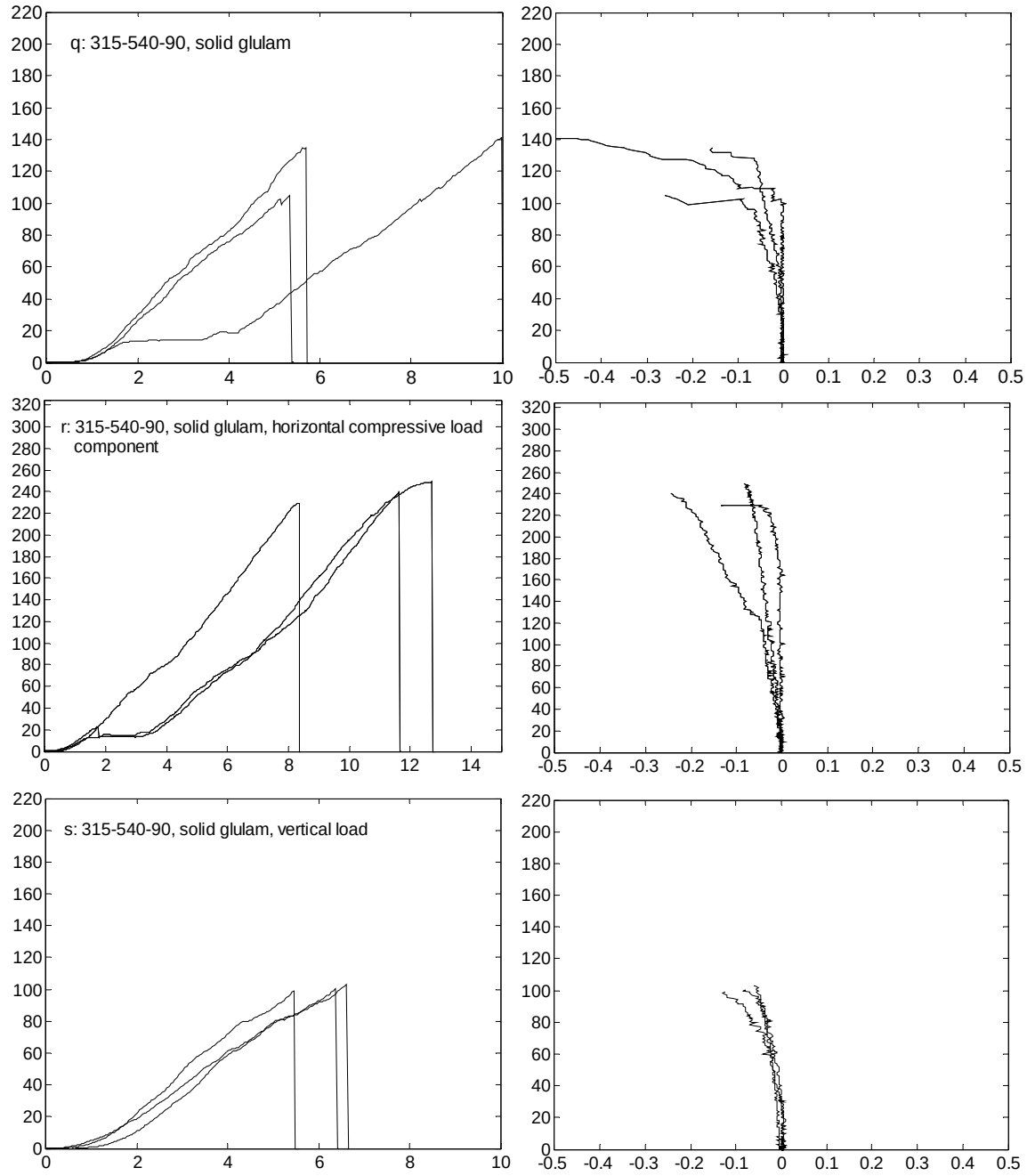

Figure 19. (5 pages). Recorded load (kN) versus global displacement (actuator stroke, mm) (left) and recorded load (kN) versus deformation (mean LVDT-gauge recording, mm) for the individual tests in the 19 test series a-s.

3.4 Some observations relating to the development of fracture

The course of fracture can for all tests be described as a sudden brittle failure exactly at the instant of peak load or a few seconds after peak load. Dependent on the crack path and action of the screws, the load could in many of the tests at the subsequent post-failure movement of the actuator be increased above the load immediately after failure. This increase reached in one of the tests in the k-series a load greater than the peak load at the instant of brittle failure.

Crackling could be heard during the course of loading, typically at two or three instances before the instant of peak load. Before peak load could in most cases a small crack be seen by the naked eye at the corner of the cleat, often just at one side of the specimen. Notes were made for a few of the tests as to the magnitude of the load when obvious crackling noise could be heard and when a crack could be seen. These notes are shown in Table 7.

Table 7. Load at observations of crackling and cracking.

Test	Load at the first crackling sound	Load at second and subsequent crackling sounds	Load at first visible crack	Failure load
b4	55 %	69 %	74 %	100 % (163 kN)
b5	61 %	69 % and 90 %	69 %	100% (130 kN)
b6	38 %	89 %	89 %	100 % (159 kN)
i1	49 %	77 %	91 %	100 % (143 kN)
k1-4	80-85 %	-	90-100 %	100% (38 kN)
Estimated typical for b	50 %	80 %	80 %	100%

For test b5 and for the tests in series k observations were made in particular as to the action of the screws. It was noted that the screws were lose with a small play between the washer and the wood just before failure. After failure the screws became active, preventing the cleat to fall off completely from the column.

Before loading was no crack visible to the naked eye observed in the vicinity of the cleat in any of the specimens. The wetting and drying of the specimens in series o and p didn't produce any crack that was observed by the naked eye.

4. Analysis of test results

4.1 Statistical significance of various parameters

The 3+3 tests b1-3 and b4-6 tested July 25 and August 28, respectively, may seem to suggest influence of different climate conditions and length of conditioning in the testing laboratory. Statistical analysis according to Wilcox's ranking method and also according to the t-distribution method show, however, that the difference is not statistically significant, it cannot with any reasonable degree of certainty be said that the strength of the specimens was influenced by the month of testing. The 6 tests in the b-series will therefore in the subsequent analysis be regarded as a sample from one single population of nominally equal specimens.

Testing of the statistical significance of observed different mean strength in different test series by means of two-sided t-testing with acceptance of 5% risk of wrong conclusion gave results that can be seen in Figure 15: any two series that don't have any overlap in the error-bars have significantly different mean strength. Thus, some of the results:

- Increased cleat thickness, h_2, decreases the load capacity of short cleats (b and c)
- Increased cleat thickness, h_2, had no significant influence for long cleats (d, e, f and g)
- Increased column depth (thickness), h_1, had no significant influence (d, e, f and g)

And moreover:

- Screws have a positive influence for virgin specimens (b and h)
- Screws had no significant influence for specimens exposed to wetting/drying (o and p)
- Tied versus untied screws had no significant influence (b and i)
- Placement of a cleat as a console at the top had no significant influence (b, l, c, m)
- Vertical global loading gives reduction of the load capacity (b and j)
- Inclined loading, 6.3^o, (tension perp. to grain) gives reduction of strength (b and k)
- Placement of cleat on side of column had no significant influence (b and n)

As a general remark: A lack of statistical significance can be due to too few tests and does not exclude the possibility of influence of the parameter under consideration.

A significant visual observation for cleats of thickness h_2=90 mm is that placement of the cleat as a console at the top of the column changes the location of the fracture, see Table 6.

The test series q-s were added for verification because of some unexpected results (series j versus b). This is discussed in greater detail in Section 4.2. These test series show:

- No significant (but possible) influence of vertical loading (q and s)
- No significant difference between glue-on cleats and solid glulam cleats (b and q)
- Inclined loading, 6.3^o, (compr. perp. to grain) gives increased strength (q, r and s)

4.2 Discussion about uncertainties. Tests for verification

4.2.1 General

From a general standpoint, uncertainty in test results can be due to: a) too small sample size, b) limited sampling range and c) various kind of inaccuracies in the testing process. In the present study there are only 3, 4 or 6 nominally equal tests in each series and the sampling range is limited by the specimens being manufactured in one plant at one instant of time, using one quality of wood and glue, and tested at one laboratory. Limited sample size can in design recommendations be considered by statistical methods, the uncertainty due to few tests being taken care of by reduced characteristic strength values. Regarding the limited sampling range it is a general requirement that application dependent estimation of representativity must be made. Here the further discussion will primarily deal only with possible inaccuracies in the testing process.

If looking at the present test results to detect any deviations or possible errors, attention is attracted to the results of series j and perhaps also to series h. If looking only at the results within each individual test series, no test result shows any obviously strange deviation although the scatter in series p, relating to specimens exposed to a wetting-drying treatment, was high, having a cov of 27%. Apart from series j and h the results of the different series don't seem to contradict general approximate expectations and neither contradict each other. Also the results of series j and h may very well be correct and representative, but are here taken as a starting point for a discussion about possible testing inaccuracies and idealizations during evaluation the test recordings.

4.2.2 Series h and influence of screws

Series h relates to the strength of specimens glued without any screws, pressure during hardening of the glue being obtained by means of clamps. The mean strength found in series h is about 30% less than that of the reference series b and the difference is statistically significant, though not very strongly. Persons with good knowledge about gluing of wood have not found the difference in strength very surprising. On the other hand is no obvious difference found between series b and n, the n-cleats being glued without screws on the side of the columns. There is furthermore no obvious influence of the screws for the specimens that were exposed to wetting and drying, see series o and p. From the testing procedure point of view there is one difference between series h and b: series h was tested July 13 while the b-specimens were tested July 25-26 and August 28, meaning somewhat different moisture conditions and time for curing of the glue. Possible influence of time is, however, contradicted by higher strength of the b-specimens tested in July and than in August. To sum up the observations, a reasonable guess may be that use of screws in fact gives a relatively higher virgin strength of specimens with a cleat placed on the narrow side of a column. Looking at the results of series o and p it seems that the increased virgin strength gained by use of screws in some cases can be lost during a wetting-drying treatment.

4.2.3 Series j and influence of global load orientation

Series j gave relatively low values of recorded strength. While about the same strength as in series b was anticipated, about 42 % lower mean strength than in b was obtained. Statistical analysis shows that the recorded difference is significant, i.e. very unlikely to be only by chance due to too few tests. The strength found in series j seems low also compared with that obtained in other series, for instance series l. Load configuration, geometry, location of fracture and recorded mean failure loads of series b, j and l are shown in Figure 20.

Various more or less likely possibilities for the results of series j can be imagined. In some way deviating manufacture process might be possible, but nothing that was obvious to observe regarding specimen appearance or course of fracture suggested any such deviation. Some gross mistake during the testing can be another possibility, but no sign or observation of any such mistake has been found except for the test result itself. A look at the dates of testing doesn't suggest that series j should deviate because of different conditioning. A different steel support arrangement, see Figure 10 and 11, at the top support was used in series j than in series b and l, but it is difficult to understand why that would be of any matter for the failure load. The support conditions of series j and l are fairly simple.

The top support arrangement for series b is somewhat more complicated and there might be a difference between the ideal action and the actual action. Resistance to rolling in the roller bearing can result in increased load carrying capacity of the cleat. Pictures of the arrangement are shown in Figures 9 and 10 and Figure 21 shows a drawing. To get a rough estimate of the rolling resistance of the arrangement with the two steel plates with two cylinders in between, it was placed on a horizontal board, carrying a weight. The board was then tilted until the cylinders started to roll. Doing this a few times it was found that the critical tilt was between 1^o and 3^o. The load when doing this simple test was only about 0.25 kN, which is very little compared to the loads at cleat testing. Assuming that rolling resistance just like friction is proportional to the normal force, the tilt found, 1^o-3^o, corresponds to friction with a coefficient of friction in the range of 0.02-0.05. No mark of any permanent plastic deformation of the steel cylinders or the steel plates was observed. However, the thin layer of corrosion protection paint on the steel parts was affected and became more and more worn and broken as tests were made.

Marks of plastic deformation were observed in the contact surface between the spherical steel part and the corresponding steel plate. It is possible that for instance the load induced tilting of the cleat load carrying surface can give some eccentricity, e, of the load. To investigate possible eccentric loading a very thin layer of ink was in some of the tests applied on the spherical steel part before testing. It was found that the centre of the contact area typically was located about 1-3 mm eccentric with respect to the centre of the cleat, but the direction of this eccentricity seemed to be at random. It can therefore be fair to assume that eccentricity contributes somewhat to scatter, but probably not giving any systematic error.

4.2.4 Verification tests. Test series q, r and s

To investigate the influence a horizontal load component and the influence of resistance to rolling of the steel cylinders in the load application setup, it was decided to do the completing test series q, r and s. The recording made at these tests have been reported in the above together the results of the basic series a-p. Comparing the results of series r and s suggests that even a small horizontal load component giving compression perpendicular to grain may have a very strong influence on the load capacity: tilting of the load by 6.3° increases the load capacity from 101 kN to 240 kN, see Table 4 and 5. The failure load in the case of using a setup with a roller support, series q, was 127 kN, suggesting existence and influence of horizontal load in the roller support.

The magnitude of the horizontal force acting across the roller support is estimated by means of a linear interpolation. A linearized failure criterion for interaction between the vertical and horizontal load components is assumed:

$$AP_{fH} + BP_{fV} = 1.0$$

where A and B are constants and P_{fH} and P_{fV} are the horizontal and vertical load components acting on the cleat at failure. For a small range of the load angle α like $0 \leq \alpha \leq 6.3^o$, a linear approximation of the actual failure criterion can be fairly accurate. The vertical and horizontal load components are related to the inclination of the load acting on the cleat according to:

$$P_{fH} = P_{fc}\sin(\alpha)\ , \quad P_{fV} = P_{fc}\cos(\alpha)$$

Knowing the magnitude of the load acting on the cleat at failure, $P_{fc} = P_f$, from tests for $\alpha=0^o$ and $\alpha=6.3^o$ A and B can be calculated. Then, by knowing the results for P_f in the case of roller support, the load inclination α_s associated with the support can be calculated. Table 8 shows the input data and the results of such calculations. In the calculations are P_{fc} made equal to the load recorded at failure, P_f, taken from Table 4. The deviation between P_{fc} and P_f is small and in the present context without any matter. The values found for α_s are of about the same magnitude as found by the simple direct tests of the roller supports, described in Section 4.2.3.

Table 8. Failure loads $P_f \approx P_{fc}$ in kN for test series with different inclination α of the load.

Inclination, α	Glued-on cleat	Solid glulam cleat	Average
0^o	97, series j	101, series s	98
Roller support	169, series b	127, series q	148
6.3^o	(240, from series r)	240, series r	240
Calculted α of the roller support, α_s	(4.6^o)	2.3^o	3.7^o

Making a combined estimation by means of the direct support tests and the estimation of Table 8 it is assumed that the non-ideal action of the roller supports used give a horizontal force corresponding to 3.0^o inclination of the load. This corresponds to a friction coefficient of magnitude 0.05. It is probable that the rolling resistance differed somewhat from one test to another test and perhaps also from one test series to another series. This means that the seemingly very strong sensitivity to a horizontal load component

contributes to the scatter in recorded strength. It is in this connection interesting to study the coefficients of variation presented in Table 4: the cov is small, 7% and 4%, for series j and s, and higher, 17% and 15%, for series b and q.

Figure 22 shows the loads acting on the cleat in the case of ideal action of the support and the result of the present estimation of the actual loads. The forces and moment shown in this figure are obtained for $\alpha_s=3.0^o$, corresponding to $\mu=\tan(3.0^o)=0.052$, and by use of the three equations of global equilibrium of the specimen. The contact area between the top of the steel sphere and the upper steel plate is assumed not to carry any moment.

2D fracture modeling and stress analysis by the finite element method and can give more information about the influence of a horizontal force. Only models that take into account only the shear stress acting across the cleat bond line are considered in the below 1D theoretical analyses. The influence of the probable deviation from ideal support action is very small in terms of shear stress.

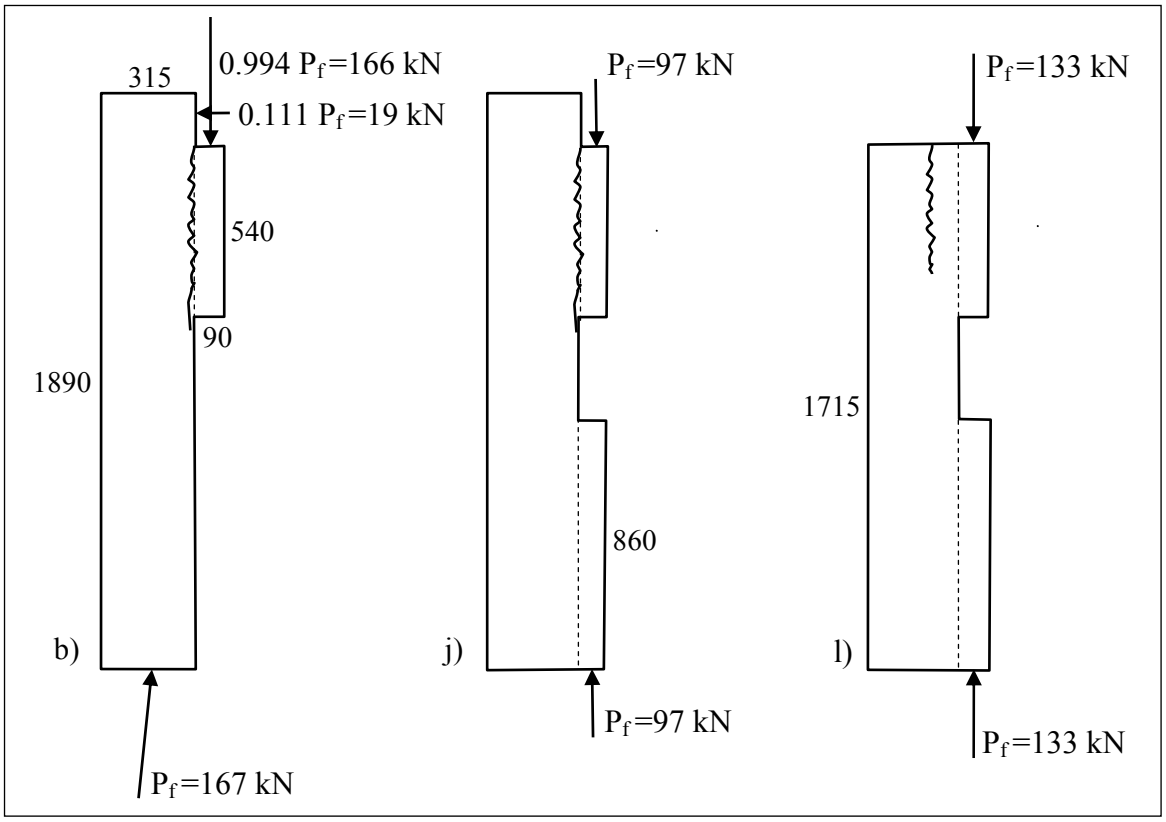

Figure 20. Specimens, fracture location and mean failure loads P_f of series b, j and l.

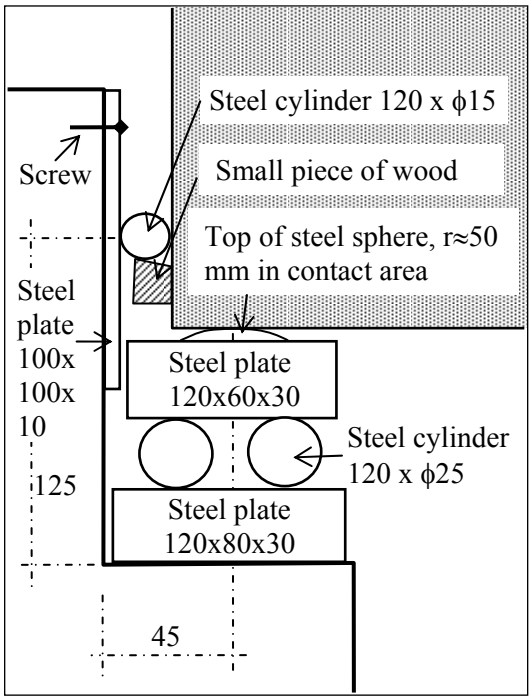

Figure 21. Support for specimens with 90 mm cleat height.

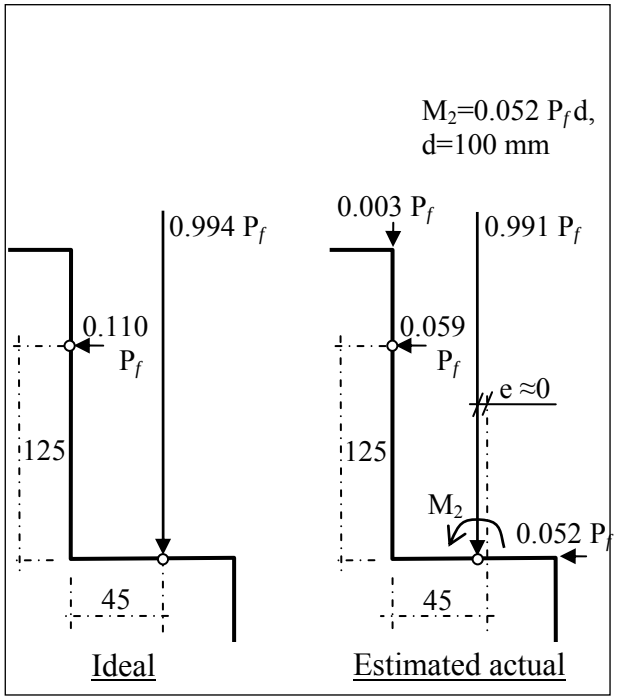

Figure 22. Forces at support. Measures valid for test series a, b, d, h, i, o, p and q.

4.3 Forces and moment acting on tested cleats at failure

The actual forces acting on the cleat at failure as estimated in Section 4.2.4 from the recorded failure loads, P_f, are indicated in Figure 23 and Table 9.

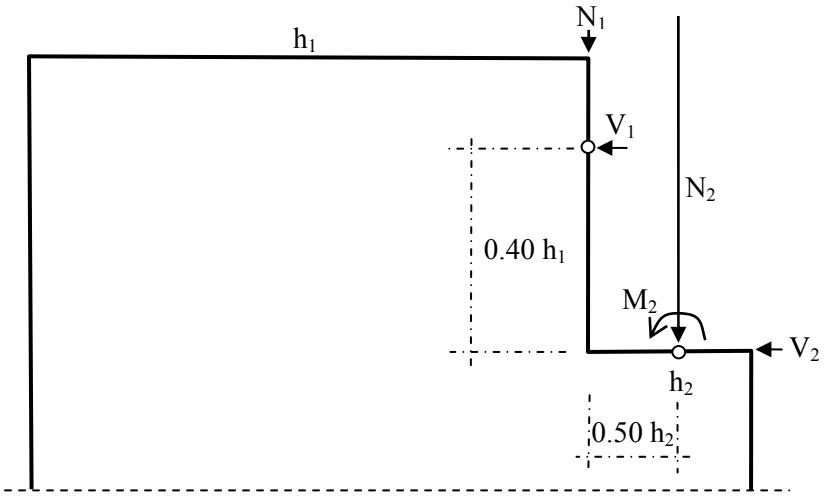

Figure 23 and Table 9. Loads acting on and in the vicinity of a cleat.

Ser.	h_1 mm	l_2 mm	h_2 mm	Mean loads and moment at failure, kN and kNm						Mean $N_2/(h_2 l_2)$ N/mm^2	Cov, %
				P_f	N_2	V_2	M_2	N_1	V_1		
a	315	270	90	48.4	48.0	2.5	0.25	0.1	2.9	1.54	5
b	315	540	90	169.5	168.0	8.8	0.88	0.5	10.0	2.70	17
c	315	540	180	86.0	85.2	4.5	0.45	0.3	5.1	1.37	13
d	315	1080	90	251.6	249.3	13.1	1.31	0.8	14.8	2.01	10
e	315	1080	180	276.7	274.2	14.4	1.444	0.8	16.3	2.21	3
f	630	1080	90	275.3	272.7	14.3	1.43	0.9	17.0	2.20	14
g	630	1080	180	269.0	266.5	14.0	1.40	0.9	16.6	2.15	12
h	315	540	90	118.3	117.2	6.2	0.62	0.4	7.0	1.89	7
i	315	540	90	174.5	172.9	9.1	0.91	0.5	10.3	2.78	13
j	315	540	90	97.3	97.3	0.0	0.00	0.0	0.0	1.57	7
k	315	540	90	38.4	38.2	- 4.2	0.00	0.0	0.0	0.61	10
l	315	540	90	133.0	133.0	0.0	0.00	0.0	0.0	2.12	9
m	315	540	180	95.2	95.2	0.0	0.00	0.0	0.0	1.52	2
n	115	540	90	189.0	187.3	9.8	0.98	0.6	11.2	3.02	10
o	315	540	90	117.8	116.7	6.1	0.61	0.4	7.0	1.88	8
p	315	540	90	129.1	127.9	6.7	0.67	0.4	7.6	2.06	27
q	315	540	90	127.0	125.8	6.6	0.66	0.4	7.5	2.03	15
r	315	540	90	239.6	238.2	26.3	2.63	0.0	0.0	3.84	4
s	315	540	90	101.0	101.0	0.0	0.00	0.0	0.0	1.63	4

4.4 Mean shear stress at failure

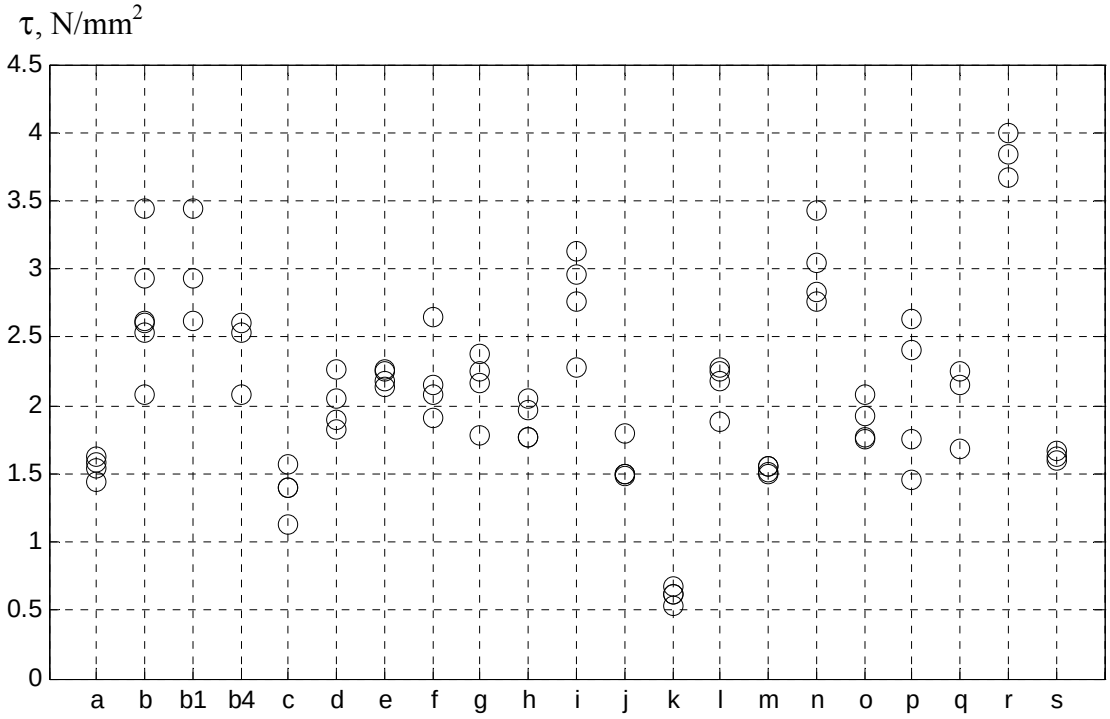

Figure 24. Mean shear stress acting on the bond area at failure for each test in series a-s.

The mean shear stress acting on the cleat bond area at failure is for the individual tests shown in Figure 24. The values shown are the force N_2 (Figure 23) at failure divided by the bond area. The mean values and the coefficient of variation for the test series are given in Table 9.

The overall mean shear stress at failure is 2.02 MPa for the entire set of 75 tests. The corresponding 5% characteristic value is 0.66 MPa. This characteristic value is determined as a value between the ranked test results 3 and 4 out of the 75 tests. These overall mean and characteristic values are of course affected by the types of loading and the types of the cleats tested.

Low mean shear stress at failure was found for

- the cleats with a low length to thickness ratio (series a, c and m)
- the specimens exposed to vertical global load (series j and s)
- the case of a horizontal tensile force component acting on the cleat (series k).

High mean shear stress at failure was found for

- the case of a horizontal compressive force component acting on the cleat (series r).

4.5 A rough estimation of characteristic load capacity of cleats

The 5% fractile characteristic strength for centric and exactly vertical cleat loading according to Figure 24 is roughly estimated means of the test results. Only geometries according to the present test specimens are considered. The width of the column and the cleat is 115 mm.

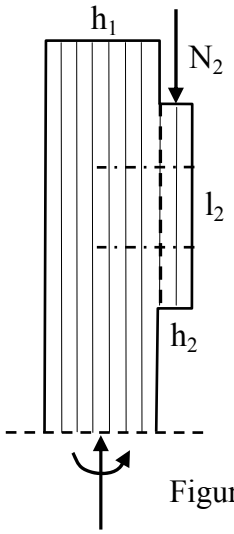

Figure 24.

The starting point for the estimations is the mean value of the vertical force N_2 at failure for the cleat geometries considered. The mean value is then adjusted according three factors representing: a) the difference between mean and characteristic value, b) the influence of the small non-zero horizontal load at the testing and c) the influence a possible wetting-drying cycle during the construction work.

The first factor is determined for normal distribution and 11.8% coefficient of variation (see Section 3.1): 1-1.64 x 0.118 = 0.81. The second factor is by means of the results of testing series b, h and s (see Table 9) estimated to be about (97.3+101.0)/(2 x 168) = 0.59. The third factor is by means of the testing results of testing series b and p (see Table 9) estimated to about 127.9/168 = 0.76. Together this gives 0.81x0.59x0.76=0.36. Since in this estimation no account is made to the uncertainty due to limited number of tests, it is fair do some rounding off downwards. The figures given in Table 10 were obtained for the factor set to 1/3 (=0.33), with mean recorded test values of N_2 from series a-g, Table 9.

In Table 10 is a comparison made with a strength design recommendation for glued lap joints given in SBI-anvisning 194 (Larsen and Riberholt, 1999). According to this recommendation is $N_{2k}=f_{vk} \times l_2 \times b$, where $f_{vk}=2.0$ MPa and with the limitation $N_{2k}\leq 100$ kN. The deviation between the experimentally based estimation and design recommendation is very big for the smaller cleats, but less for large cleats due to the 100 kN limit.

Table 10. Characteristic strengths as estimated from tests and according to a design code.

Dimensions			Characteristic values: N_{2k} (kN) and mean shear stress f_{vk} (MPa)			
			From the present tests		Acc. to SBI-anvisning 194	
h_1 mm	l_2 mm	h_2 mm	N_{2k} (kN)	f_{vk} (MPa)	N_{2k} (kN)	f_{vk} (MPa)
315	270	90	16	0.52	62	2.00
315	540	90	56	0.90	100	-
315	540	180	28	0.46	100	-
315	1080	90	83	0.67	100	-
315	1080	180	91	0.74	100	-
630	1080	90	91	0.73	100	-
630	1080	180	89	0.71	100	-

4.6 Local shear stress at failure according 1D shear slip analysis

4.6.1 Method of analysis

The shear stress distribution along the bond line is calculated according (Volkersen, 1938) with the shear stiffness of the shear layer that models the bond line determined according to fracture mechanics so that the fracture energy and the local shear strength of the bond line are reproduced correctly (Gustafsson, 1987). The two wooden parts, i.e. the cleat and the column, are assumed to act as two linear elastic bars. Any bending stress or deformation is not considered. The bond line is modeled as a linear elastic shear stress-slip layer. Normal tensile or compressive stresses acting across the bond area are not considered.

The loading configuration affects the calculated shear stress distribution. Figure 25 shows for a certain geometry and material parameters the shear stress distribution for a configuration where both the column and the cleat are in compression and for a configuration where the cleat is in compression and the column is in tension. These two configurations are here called compression-compression, C/C, and pull-compression, P/C. All test series expect k relate to load configuration C/C. The specimens in series k were loaded in P/C.

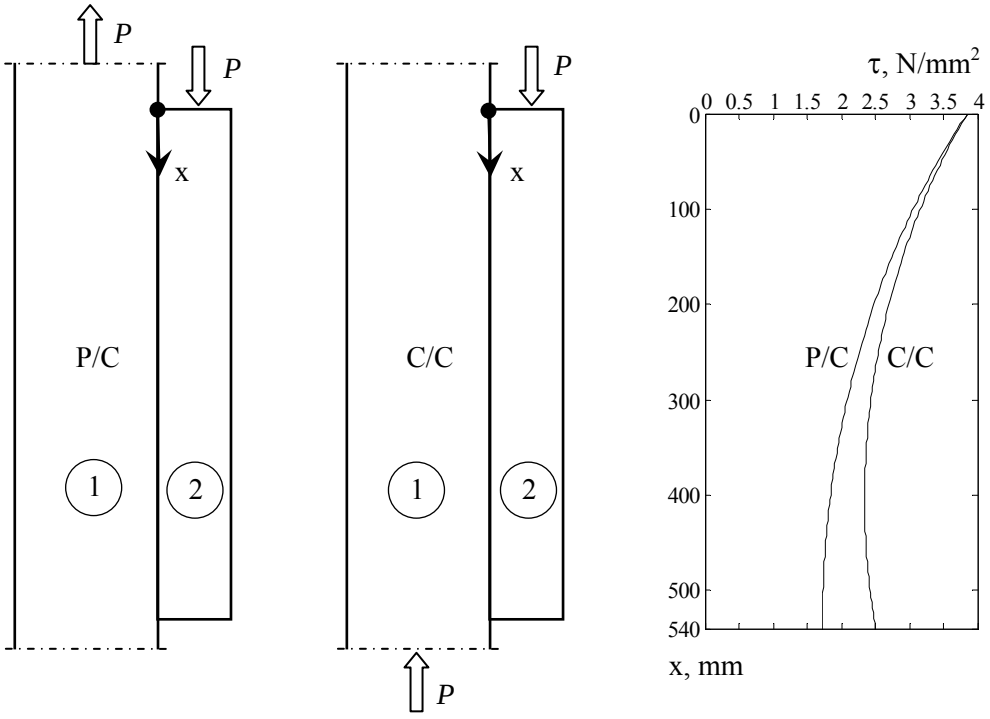

Figure 25. Load configurations and stress distribution.

Equations for shear stress distribution, maximum stress and failure load are derived and presented in the Appendix "1D stress and strength analysis of lap joints". Maximum shear stress is found at x=0 for both P/C and C/C if the normal stiffness of the column cross section area, E_1A_1, is greater than that of the cleat, E_2A_2. For loading condition C/C is the maximum shear stress:

$$\tau_{\max} = \frac{P\omega}{b_3}\left(\frac{1}{E_1A_1}+\frac{1}{E_2A_2}\right)^{-1}\left(\frac{1}{E_1A_1\sinh(\omega l)}+\frac{1}{E_2A_2\tanh(\omega l)}\right)$$

and for loading condition P/C:

$$\tau_{\max} = \frac{P\omega}{b_3}\frac{1}{\tanh(\omega l)}$$

where

$$\omega = \sqrt{\frac{f_v^2 b_3}{2G_f}\left(\frac{1}{E_1A_1}+\frac{1}{E_2A_2}\right)}$$

where b_3 is the width of the glued area, f_v is the local shear strength of the bond line and G_f is the fracture energy of the bond line. Both f_v and G_f are in general affected both by the properties of the wood and by the properties of the glue. G_f can be strongly affected by the glue properties also in cases where the fracture takes place in the wood in the vicinity of the glue line. Youngs modulus is in the present application equal for the column material and the cleat material, that is $E_1 = E_2 = E_0$, where E_0 is the modulus of elasticity along the grain of the wood.

The for fracture criterion for calculation of the failure load can be expressed in terms of shear stress as

$$\tau_{\max} = f_v$$

or, alternatively, in terms energy release $\mathcal{G}$ rate as

$$\mathcal{G} = G_f ,$$

the two alternatives giving the same result due to the special choice of bond line stiffness. The material quantities that govern the failure load are thus f_v, $(E_1G_f)/f_v^2$ and E_1/E_2. In the present application is $E_1/E_2 = 1.0$ throughout. Accordingly two material quantities are of interest: f_v and $(E_1G_f)/f_v^2$. In a study (Gustafsson and Serrano, 1998) of test results (Glos and Horstman, 1989) material data were obtained by fitting of the failure loads predicted by the present theory to the corresponding experimental failure loads of various glued lap joints loaded in the P/C load configuration. The wood material was spruce and three kinds of glue were tested: R/P, Epoxy and PVAc. The values of f_v and E were assumed to be the same for all specimens regardless of type of glue. The material data that were found are shown in Table 11.

Table 11. Strength and fracture material data.

Adhesive	R/P	Epoxy	PVAc
G_f, Nmm/mm^2	0.80	1.40	1.60
E, N/mm^2	11000	11000	11000
f_v, N/mm^2	3.85	3.85	3.85
EG_f/f_v^2, *mm*	594	1039	1187

The glue used in the present tests of cleats was polyurethane (series a-p) and melamine (series q-s). It is in the present analysis of test results assumed that the material property length $(E_1 G_f)/f_v^2$ for the present combination of glue and wood is 1000 mm. This is an approximate average of the values for R/P, Epoxy and PVAc. For E=11000 N/mm^2 and f_v=3.85 N/mm^2 it corresponds to G_f =1.35 Nmm/mm^2, which is about the same or somewhat higher than values that commonly are considered as typical for solid spruce wood.

4.6.2 Predicted failure loads and local shear stress at failure

The shear strength f_v obtained from experimentally found failure loads are for $(E_1 G_f)/f_v^2 = 1000$ mm indicated in Figure 26.

The failure loads predicted by means of the strength equations in Section 4.6.1 with $(E_1 G_f)/f_v^2 = 1000$ mm and $f_v = 3.85$ N/mm^2 are indicated in Table 12 as the ratio between the theoretically predicted value of force N_2 (defined in Figure 23) at failure and experimental value of N_2 at failure, given in Table 9.

The very different values of f_v found in the different test series is most probably reflecting influence of perpendicular to grain normal stress in the fracture region. Significant normal stresses can be expected in particular for short thick cleats. The present theory is a shear theory and is at first hand useful for slender lap joints in which joint bending and bond line normal stress are negligible and the shear stress is predominant. Slender joints with relatively small bending effects are represented by test series d and f. The very good agreement between test and theory for the reference test series b can be by chance, reflecting similarity in some sense between the series b and the tests presented in (Glos and Horstman, 1989).

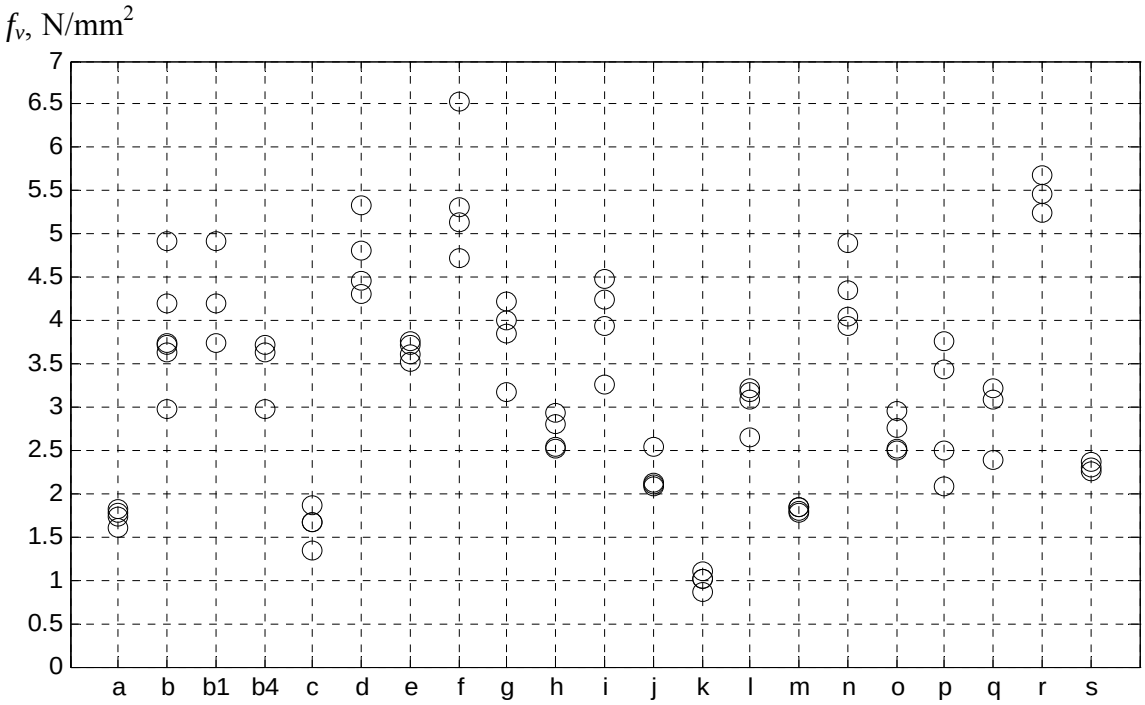

Figure 26. Maximum local shear stress in tested specimens at failure acc. to a theory.

Table 12. Ratio $N_{2f,theory}/N_{2f,test}$ for f_v=3.85 MPa and $(E_1 G_f)/f_v^2 = 1000$ mm.

Ser.	h_1 mm	l_2 mm	h_2 mm	N_{2f} Test kN	Remark	N_{2f} Theory/Test -
a	315	270	90	48.0	Shorter cleat	2.23
b	315	540	90	168.0	Reference case	1.01
c	315	540	180	85.2	Thicker cleat	2.37
d	315	1080	90	249.3	Longer cleat	0.82
e	315	1080	180	274.2	Longer thicker cleat	1.06
f	630	1080	90	272.7	Longer cleat on larger column	0.72
g	630	1080	180	266.5	Longer thicker cleat on larger column	1.02
h	315	540	90	117.2	No screws	1.44
i	315	540	90	172.9	Screws not untied	0.98
j	315	540	90	97.3	Vertical load	1.74
k	315	540	90	38.2	Tensile load comp. Column in tension	3.87
l	315	540	90	133.0	Cleat at top of column. Vertical load	1.27
m	315	540	180	95.2	Thicker cleat at top. Vertical load	2.12
n	115	540	90	187.3	Cleat placed on column side	0.90
o	315	540	90	116.7	Wetting-drying. No screws	1.45
p	315	540	90	127.9	Wetting-drying. With screws	1.32
q	315	540	90	125.8	Solid glulam	1.34
r	315	540	90	238.2	Solid glulam. Compr. load comp.	0.71
s	315	540	90	101.0	Solid glulam. Vertical load	1.67

5. Concluding remarks

The load carrying capacity of cleats can be strongly affected by choice of design and mode of loading, and the capacity can be made very high, provided proper design. Even a comparatively small load component perpendicular to the cleat may affect its load capacity very much, in a positive or negative way, depending on the direction of the load.

Strength analysis at the assumption of uniform shear stress and no influence of normal stress can in general not be expected to give valid results, but may be used for making simple reference calculations. 1D fracture mechanics analysis in which only the shear stress is considered may give valid results in the case of very slender cleats loaded by a shear load. 2D fracture mechanics analysis is most probably needed for accurate results in more general cases.

The strength performance of conventionally glued cleats is characterized by stress concentration and a brittle material behavior. One consequence of this is that the load capacity is not proportional to the structural size, as is evident from the present test results. Another consequence, not studied here, is possible sensitivity to impact loading. The possible sensitivity to impact loading, the load capacity not being proportional to size, sensitivity to moisture gradient induced imposed deformations and the sensitivity to tensile normal stress might be overcome by means of measures that reduce the stress concentration and the brittle material performance. Such a measure might be use of a compliant bond achieved by having a rubber layer glued in between the two wooden parts.

Literature references

Glos, P. and Horstman, H. (1989): “Strength of glued lap timber joints”, Proceedings of CIB-W18A Meeting 22, East Berlin, 1989, paper 22-7-8, pp. 1-17

Gustafsson, P.J. (1987): “Analysis of generalized Volkersen joints in terms of non-linear fracture mechanics”, In proc. of European Mechanics Colloquium 227 “Mechanical behavior of adhesive joints”, St. Etienne, France, 1987, pp. 323-338.

Gustafsson, P.J. and Serrano, E. (1998): “Glued truss joints analyzed by fracture mechanics”, In proc. of the 5th World Conference on Timber Engineering, Montreaux, Switzerland, 1998 vol. 1, pp. 257-264.

Larsen, H.J. and Riberholt, H. (1999): “Träkonstruktioner. Förbindelser”, SBI-anvisning 194, SBI, Denmark, 1999, pp. 106-107

Volkersen, O. (1938): ”Die Nietkraftverteilung in zugbeanspruchten Nietverbindungen mit konstanten Laschenquerschnitten”, Luftfahrtvorschung, Band 15, pp. 41-47

Appendix:

1D stress and strength analysis of lap joints

1. Assumptions and notations

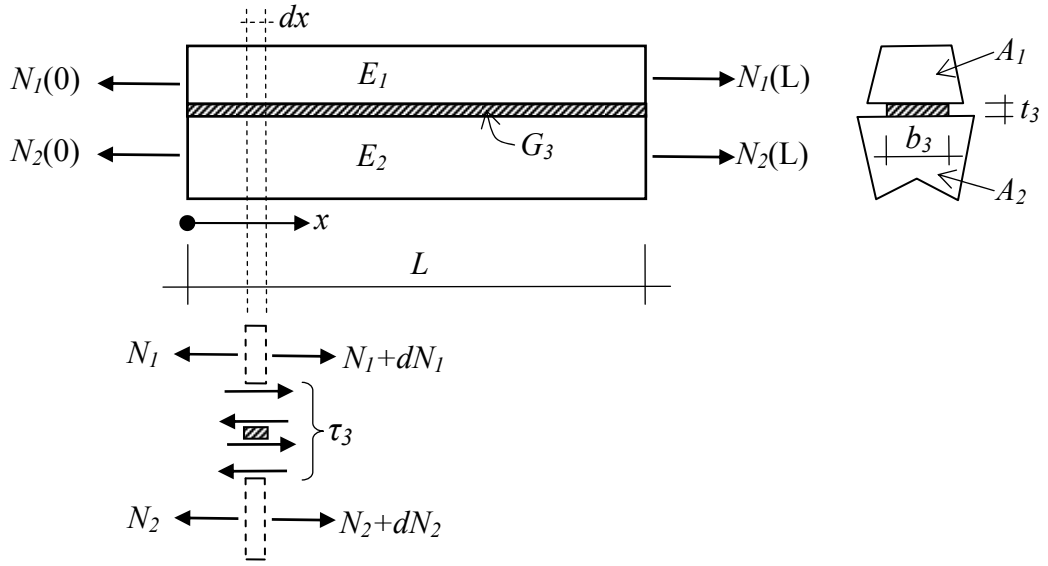

The kind of adhesive lap joint under consideration is shown in the above figure. It is made up of two adherends denoted 1 and 2 and an adhesive layer denoted 3. The adherens are assumed to act as linear elastic centrically loaded bars. The adhesive layer in between the bars is assumed to act as a linear elastic layer that deforms only in shear with constant shear strain across the bond layer thickness t_3. The adherend cross section areas A_1 and A_2, the bond layer cross section dimensions t_3 and b_3, and also the material stiffness parameters E_1, E_2 and G_3 are all assumed to be constant with respect to the location x along the joint. The bars are assumed not to bend and any influence of possible normal stress in the bond layer is disregarded.

The normal stress in the two adherens is denoted $\sigma_1 = N_1/A_1$ and $\sigma_2 = N_2/A_2$, respectively. The shear stress in the adhesive layer is denoted τ_3. The corresponding normal and shear strains are denoted ε_1, ε_2 and γ_3. Adherend displacements are indicated by u_1 and u_2. The stresses, strains and displacements are all functions of the location x. Derivative with respect to x is indicated by ′, that is, as an example, $\sigma_1' \equiv d\sigma_1 / dx$.

2. Governing equation

Equilibrium of the two parts of length dx gives

$$\begin{cases} dN_1 + \tau_3 b_3 dx = 0 \\ dN_2 - \tau_3 b_3 dx = 0 \end{cases} \tag{1}$$

which by division by $A_1 dx$ and $A_2 dx$, respectively, give:

$$\begin{cases} \sigma_1' + (b_3 / A_1)\tau_3 = 0 \\ \sigma_2' - (b_3 / A_2)\tau_3 = 0 \end{cases} \tag{2}$$

The shear strain γ_3 is assumed to be constant across the thickness of the adhesive layer. By this assumption and by use of the conventional definitions of shear strain and normal strain:

$$\begin{cases} \gamma_3 = (u_2 - u_1) / t_3 \\ \varepsilon_1 = u_1' \\ \varepsilon_2 = u_2' \end{cases} \tag{3}$$

The materials are assumed to be linear elastic:

$$\begin{cases} \tau_3 = G_3 \gamma_3 \\ \sigma_1 = E_1 \varepsilon_1 \\ \sigma_2 = E_2 \varepsilon_2 \end{cases} \tag{4}$$

Derivation of (3a) twice and then substitution first by (3b) and (3c), then by (4) and finally by (2) give:

$$\tau_3'' - \omega^2 \tau_3 = 0 \quad \text{where} \quad \omega^2 = (G_3 b_3 / t_3)\ (1/(A_1 E_1) + 1/(A_2 E_2)) \tag{5}$$

This second order homogeneous ordinary linear differential equation with constant coefficients governs the shear stress distribution and it has the solution

$$\tau_3 = C_1 \cosh(\omega x) + C_2 \sinh(\omega x) \tag{6}$$

Eq (5) was derived by Volkersen in 1938 in relation to analysis of the load distribution in riveted lap joints (Volkersen, 1938). Eq (5) shows that the normalized joint length parameter ωL, often used in lap joint analysis, is:

$$\omega L = L\sqrt{\frac{G_3 b_3 (1+\alpha)}{t_3 E_1 A_1}} \quad \text{where} \quad \alpha = (E_1 A_1)/(E_2 A_2) \tag{7}$$

3. Determination of integration constants

The constants C_1 and C_2 can be obtained from boundary conditions in terms of the normal forces $N_1(0)$, $N_2(0)$, $N_1(L)$ and $N_2(L)$. This requires that normal the forces in the two adherends are related to the shear stress, τ_3. Derivation of (3a) and then use of (3b) and (3c) give:

$$\varepsilon_2 - \varepsilon_1 = t_3 \gamma_3' \tag{8}$$

which by means of (4) gives

$$\frac{N_2}{E_2 A_2} - \frac{N_1}{E_1 A_1} = \frac{t_3}{G_3} \tau_3' \tag{9}$$

By use of (6) it is then found that for every location x is

$$C_1 \sinh(\omega x) + C_2 \cosh(\omega x) = (G_3 / (t_3 \omega))\ (N_2(x) / E_2 A_2 - N_1(x) / E_1 A_1) \tag{10}$$

Knowing the normal forces at x=0 and x=L, a system of two equations is obtained from which the coefficients C_1 and C_2 can be calculated:

$$\begin{bmatrix} 0 & 1 \\ \sinh(\omega L) & \cosh(\omega L) \end{bmatrix} \begin{bmatrix} C_1 \\ C_2 \end{bmatrix} = G_3 / (t_3 \omega) \begin{bmatrix} N_2(0) / E_2 A_2 - N_1(0) / E_1 A_1 \\ N_2(L) / E_2 A_2 - N_1(L) / E_1 A_1 \end{bmatrix} \tag{11}$$

By solving this equation the constants are found to be:

$$\begin{cases} C_1 = (G_3 / (t_3 \omega)) \left(\dfrac{-\left(N_2(0) / E_2 A_2 - N_1(0) / E_1 A_1\right)}{\tanh(\omega L)} + \dfrac{\left(N_2(L) / E_2 A_2 - N_1(L) / E_1 A_1\right)}{\sinh(\omega L)} \right) \\ C_2 = (G_3 / (t_3 \omega)) \left(N_2(0) / E_2 A_2 - N_1(0) / E_1 A_1\right) \end{cases} \tag{12}$$

4. Shear stress at load condition pull-pull

The special loading condition "pull-pull" corresponds to $N_1(0) = N_2(L) = P$ and $N_1(L) = N_2(0) = 0$, which by (12) give the constants C_1 and C_2 as

$$\begin{cases} C_1 = PG_3/(t_3\omega)\left(1/\left(E_1A_1\tanh(\omega L)\right)+1/\left(E_2A_2\sinh(\omega L)\right)\right) \\ C_2 = PG_3/(t_3\omega)\left(-1/E_1A_1\right) \end{cases} \tag{13}$$

that inserted in (6) give the shear stress distribution for this type of loading. Max shear stress $\tau_{3,max}$ is found at $x=0$ if the notation of the adherends is made so that $E_1A_1 \le E_2A_2$. Accordingly, by means of (6) and (13) is

$$\tau_{3,\max} = PG_3/(t_3\omega)\left(1/\left(E_1A_1\tanh(\omega L)\right)+1/\left(E_2A_2\sinh(\omega L)\right)\right) \tag{14}$$

5. Shear stress at load condition pull-compression

The special loading condition "pull-compression" corresponds to $N_1(0) = -N_2(0) = P$ and $N_1(L) = N_2(L) = 0$, which by (12) gives the constants as

$$\begin{cases} C_1 = PG_3/(t_3\omega)\left(1/E_1A_1+1/E_2A_2\right)/\tanh(\omega L) \\ C_2 = PG_3/(t_3\omega)\left(-1/E_1A_1-1/E_2A_2\right) \end{cases} \tag{15}$$

that inserted in (6) give the shear stress distribution for this type of loading. Max shear stress is found at $x=0$ if the notation of the adherends is made so that $E_1A_1 \le E_2A_2$. Accordingly, by means of (6) and (15) is

$$\tau_{3,\max} = PG_3/(t_3\omega)\left(1/E_2A_2+1/E_1A_1\right)/\tanh(\omega L) \tag{16}$$

6. Fracture mechanics properties of adhesive layer

The local shear strength of the layer is denoted f_v and its shear fracture energy is denoted G_f. Shear stress versus shear deformation of the layer is assumed to be linear and therefore the fracture energy of the layer can be calculated as the stress at failure, f_v, times the relative shear displacement at failure, $t_3\gamma_{3f}$, divided by 2:

$$G_f = \frac{\tau_f (t_3 \gamma_{3f})}{2} = \frac{\tau_f^2 (t_3 / G_3)}{2} \tag{17}$$

where $\gamma_{3f} = f_v / G_3$ is the shear strain at failure. This means that ratio G_3/t_3 can be replaced according to

$$G_3 / t_3 = \frac{f_v^2}{2G_f} \tag{18}$$

For a bond layer that in fact performs in an ideal linear elastic brittle manner, it does not matter whether G_3 or G_f is used for characterization of the bond layer properties. For real materials, results much closer to reality are obtained if using G_f instead of G_3 when strength properties are analyzed. G_f gives an integral mean value kind of characterization of fracture ductility while G_3 give a good representation only of the first stiff and linear part of the bond layer performance. Replacement of G_3 / t_3 with $f_v^2 /(2G_f)$ was proposed in (Gustafsson, 1987). Using this substitution, the normalized joint length parameter ωL given in (7) can be written as

$$\omega L = L\sqrt{\frac{f_v^2 \, b_3 (1+\alpha)}{2G_f E_1 A_1}} \quad \text{where} \quad \alpha = (E_1 A_1)/(E_2 A_2) \tag{19}$$

7. Failure criterion

If choosing the bond layer shear stiffness G_3 in calculations according to (18), then the stress criterion

$$\tau_{3,\max} = f_v \tag{20}$$

and the energy criterion

$$\mathcal{G} = G_f \tag{21}$$

where $\mathcal{G}$ is the energy release during crack extension, give the same predicted failure load.

8. Failure load at load condition pull-pull

The criterion (20) together with (14) and (19) gives:

$$P_{failure} = (b_3 L f_v)\,\frac{(1+\alpha)\sinh(\omega L)\tanh(\omega L)}{\omega L\big(\sinh(\omega L)+\alpha\tanh(\omega L)\big)} \tag{22}$$

where

$$\alpha = E_1 A_1 / E_2 A_2 \le 1 \tag{23}$$

Since $\tanh(\omega L)$ approaches 1.0 for large ωL, for large ωL it is found that

$$P_{failure} \approx (b_3 L f_v)\,\frac{(1+\alpha)}{\omega L} \tag{24}$$

This approximation deviates less than 0.5% from the exact value when the normalized joint length $\omega L \ge 6$.

Since shear strength is independent of sign, the same joint strength prediction is obtained for loading compression-compression as for pull-pull.

9. Failure load at load condition pull-compression

The criterion (20) together with (16) and (19) gives:

$$P_{failure} = (b_3 L f_v)\,\frac{\tanh(\omega L)}{\omega L} \tag{25}$$

where α and ωL are defined in (23) and (19).

It can be observed that the failure loads for load conditions pull-pull and pull-compression are approximately the same for small α and coincide when $\alpha \to 0$.

Since $\tanh(\omega L)$ approaches 1.0 for large ωL, for large ωL it is found that

$$P_{failure} \approx (b_3 L f_v)\,\frac{1}{\omega L} \tag{26}$$

This approximation deviates less than 0.5% from the exact value when the normalized joint length $\omega L \ge 3$.

10. Failure load diagram

The below diagram shows the failure load in terms $P_{failure}/(b_3 L f_v)$ versus the dimensionless number ωL for loading conditions pull-pull and pull-compression at various value of the adherend normal stiffness ratio α. Loading condition compression-compression gives the same predicted failure load as pull-pull. ωL and α are according to (19) and (23):

$$\omega L = L\sqrt{\frac{f_v^2 b_3(1+\alpha)}{2G_f E_1 A_1}} \quad \text{and} \quad \alpha = (E_1 A_1)/(E_2 A_2) \le 1.0$$